Combined responses to reviewers

1 Response to General Comments

General comments by both reviewers begin with accurate and concise summaries of the work presented. We appreciate their careful reading of our manuscript and insightful suggestions. Changes to the manuscript detailed below refer to the "markup document" which is the latexdiff outputted text attached to this document.

Our response in this section addresses the following statements by Referee #1.

Comment, Ref. 1: **The verity of model results presented in the study depends partially on the accuracy of the improved solar transmission parameterization presented in Section 2.1 of the manuscript. The "base-case" solar transmission parameterization can be traced back to data and curve fitting given in Morel (1988). The "new" solar transmission parameterization (given in Section 2.1 of the manuscript that explicitly includes CDM) is not however thoroughly presented. The reader is only told the new parameterization is "the best fit function" to "244 concurrent measurements". Quantitative information about the goodness of fit is not presented. Nor is the true number of degrees of freedom (perhaps something like 8 given the very limited spatial distribution of observations) discussed. Therefore, the reader can't judge the quality of the "new" parameterization and its appropriateness for a global model.**

Markup document: Page 8, lines 8-18 & Page 30, Fig. 2
In developing a new optical parameterization, the parameters for the best fit function to the k_d, chlorophyll-a and CDM data were found by minimizing the least squares distance between modeled and measured values using the Levenberg-Marquardt algorithm, which is now mentioned in the text. We also discuss the results of a sensitivity analysis that addresses the limited spatial distribution of observations.

Markup document: Page 8, lines 19-20 & Page 32, Fig. 4
Goodness of fit between the parameterized k_d values and the observed are shown in Figure 4, panels (a) and (b). The color scheme matches locations according to a revised map of data stations (Figure 2).

Markup document: Page 22, lines 5 - 9
The issue of limited spatial representation of the new parameterization is included in our discussion of assumptions and simplifications in the Conclusion section.

Comment, Ref. 1: **The manuscript title that begins "A new parameterization for surface ocean light attenuation" doesn't accurately reflect the paper content. The parameterization is explained in less than a page and supported by only a single figure (Figure 2). In situ data that validate the parameterization (or not) are never presented. A very first logical step in parameterization development would be to address the validity of a correlation between chlorophyll**

concentration and CDM, as the "chlorophyll only" parameterization considered in the study may implicitly include CDM (according to Morel 1988 the parameterization includes the influence of chlorophyll "and co-varying material"). Before explicitly including CDM it should be shown that it does not truly co-vary with Chl. The NOMAD data presented in the study easily allow for this. The study seems more of a numerical exploration of how ocean biogeochemistry could change if models considered slightly more solar attenuation that may be attributed to underestimating the influence of CDM in existing parameterizations. Such a numerical exploration is still interesting, novel, and has scientific merit.

Markup document: Page 1
We agree that the main focus of the content in our paper and title are somewhat misaligned. The main focus of the study is the biological impact of adding more light attenuation in an ESM, rather than the new parameterization. The new title our study is "Quantifying the biological impact of surface ocean light attenuation by colored detrital material in an ESM using a new optical parameterization". The new running title is: "Biological impact of increased light attenuation by CDM in an ESM".

Markup document: Page 8, lines 19-20 & Page 32, Fig. 4
In situ data validation is now shown in Figure 4.

Markup document: Page 8, lines 7-8 & Page 31, Fig. 3
Per the reviewer's suggestions, we provide additional details about the new parameterization used in this paper. We motivate the need for this new parameterization with Figure 3, which shows that chlorophyll-a and light absorption by colored detrital matter at 443nm, $a_{dg}(443)$, are uncorrelated for the subset of NOMAD data used in this analysis. These data meet the following criteria: (1) measurements of chlorophyll-a, light absorption by CDM and the diffuse attenuation coefficient for downwelling irradiance, k_d, were made concurrently and (2) chlorophyll-a data are derived from HPLC analysis. We restricted our analysis to samples analyzed by HPLC to use data derived from a consistent method of measurement.

Comment, Ref. 1: **Restating the above paragraph more succinctly, if a "new parameterization" (implied by the word "new" to be better than existing) is a goal of the study, then the paper would benefit from a much more through motivation, presentation, discussion and validation of the parameterization itself. If the focus is Earth system and biogeochemical model results considering two different parameterizations (the way the paper reads now), the paper would benefit from backing off on promoting a "new parameterization".**

We believe to have sufficiently addressed these comments by changing the manuscript title and providing additional details about the parameterization as shown above.

2 Response to Specific Comments

Comment, Ref. 2: **The Abstract needs to be rearranged to convey the most important findings of the paper and the assumptions/limitations used. Important findings are the decoupling of surface nutrients and surface biomass as well as the fact that light limitation affects differently the surface and the total productivity. Important assumption is that of a unique relationship (equation 5) imposed on all of the biomes. Important limitations are the small amount of data the empirical relationship is based on and the fact that the adg used in the model is fixed in time.**

Markup document: Pages 2 - 3
We agree that the abstract should highlight the important findings and assumptions as the reviewer mentioned. The abstract was edited accordingly.

Comment, Ref. 1: **Pg 3907, Line 20. Technically the sentence should read "implicitly includes the light attenuation of all other aquatic constituents presumed to be directly in proportion with Chlorophyll".**

Markup document: Page 4, lines 4 - 5
We changed the wording exactly as suggested.

Comment, Ref. 1: **Pg 3909, Line 6. Sentence indicates "variations in light attenuation in ESMs were previously attributed to phytoplankton pigment only". However this is not technically true as pointed out by the authors (See pg 3907, lines 19-20, also Jerlov 1976 and Morel 1988).**

Markup document: Page 5, lines 12 - 14
We changed this wording to "Variations in light attenuation in ESMs were previously attributed to chlorophyll and implicitly to aquatic constituents assumed to vary in proportion to chlorophyll."

Comment, Ref. 1: **Pg 3909, Line 19 CDOM only absorbs solar radiation within a small portion of the solar spectrum (i.e. the UV and blue wavebands). Suggesting that CDOM "accounts for a large fraction of the non-water absorption 'especially' in the UV and blue wavelengths" seems misleading. It is really 'only' in the UV and blue wavelengths.**

Markup document: Page 5, line 25
We removed the word "especially".

Comment, Ref. 2: **The Introduction would benefit by an extra paragraph that describes the results by Siegel et al 2005 with regards to the distribution of CDOM in open vs coastal waters, equatorial vs high latitudes. Siegel et al 2005 show that most of the signal from CDOM is in coastal waters. The implicit reason for discussing the regional dependence is to set the stage for qualifying the parameterization described in the next section.**

Markup document: Page 6, lines 9 - 12

We agree the results from Siegel et al (2005) are relevant to this paper and are included in our discussion of the bio-optical assumption at the end of the Introduction section.

Markup document: Page 9, lines 19 - 21
We qualified the parameterization by stating that region-specific optical relationships are not captured by this single global parameterization.

Comment, Ref. 1: **Pg 3910, Line 25 The reason CDOM isn't included in the Kd(r) parameterization isn't because CDOM absorption in red wavelengths is smaller than in blue-green wavelengths, it's because CDOM absorption in red wavelengths is extremely small compared to absorption by seawater and chlorophyll in the red wavelengths.**

Markup document: Page 7, lines 14 - 16
We changed the text to reflect this.

Markup document: Page 29, Fig. 1
We also included the median absorption by particles (including phytoplankton) from the NOMAD dataset and the absorption spectrum of water to Figure 1 from Pope and Fry (1997).

Markup document: Page 24, lines 32-33
We added Pope and Fry (1997) to the bibliography.

Comment, Ref. 1: **Figure 2 The comparison of Equations 3 and 5 applied to NOMAD data could be clarified. First, given the NOMAD data are from 8 locations, coloring the data by location would help the reader interpret the true number of degrees of freedom. Second, the distribution looks extremely bimodal. If a handful of outlying points were removed the regression line looks like it would have a slope very near 1.0. It would be interesting to know the location of data points that fall well below the 1:1 line. Again, this could be indicated by color coding.**

Markup document: Page 8, lines 2 - 7 & Page 30, Fig. 2
In response to the reviewer's comments, we provide a color-coded map of station locations. We separate the observational data into 7 categories: (1) western Atlantic, northern cluster in black; (2) western Atlantic, southern cluster in green; (3) Antarctic peninsula in orange; (4) Southern Ocean in blue; (5) western Pacific in magenta; (6) stations across the Pacific ocean in red and (7) eastern Pacific in cyan.

Markup document: Page 32, Fig. 4 panel (c)
The points on this plot are now color coded following the same color scheme as Fig. 2. The locations of points that fall below the regression line are mostly black, green and cyan representing three different location clusters from the dataset.

Comment, Ref. 2: **The new parameterization, Equation (5), is obtained after all the data from NOMAD with concurrent values of kd, chl and adg are plotted in a single plot and fitted by a least-squares regression. However, inspection of Figure 2 shows that most of the data points**

are in very specific areas, not representative of the global ocean. For example, coastal upwelling regions, Arctic Ocean as well as the open ocean are underrepresented. Of course, this is inevitable, given the few data points where concurrent measurements exist, hence not a criticism here. However, I suggest the authors discuss the validity of (5) doing some quick sensitivity analysis. For example, if they removed from their regression fitting a group of values at a time, eg the Southern Ocean, or the Amazon outflow, would they get very different coefficients in (5)? In this manner, they can assess how important each region is for obtaining the parameters in Equation (5).

Markup document: Page 8, lines 14 - 18
We conducted the exercise suggested by the reviewer. We removed the following clusters of points from the regression fitting to test the sensitivity of the parameterization to the data from each region: (1) north Atlantic; (2) Amazon River outflow and nearby offshore stations; (3) Antarctic peninsula; (4) Southern Ocean; (5) western Pacific; (6) stations across the Pacific ocean and (7) eastern Pacific. These clusters correspond to the color-coded spatial groupings shown in Figure 2. The parameters are mostly stable. The only parameter whose change was well outside the fitting variability was the exponent to the chlorophyll term, which increased by 0.23 when the eastern Pacific stations were omitted. We added this information to the manuscript.

Comment, Ref. 2: **Section 2.2, lines 9-11. It is unclear to me whether the present model configuration allows for changes in climate (SST) due to changes in chlorophyll distribution which in turn result from differential light absorption. Please clarify. This will affect the discussion of biomes later on.**

Markup document: Page 9, lines 13 - 19
The same optical model is used for calculating light attenuation for physics and biology in our ESM configuration. Therefore, the same attenuation depth is used in evaluating physical processes (such as the surface shortwave heating flux) and biological productivity (by setting the euphotic depth for phytoplankton). The optical model calculates light attenuation using model-derived chlorophyll concentration. Increases in chlorophyll concentration will reduce the attenuation depth, reducing total light available for photosynthesis and the total shortwave heating of the ocean. We expanded on this point to make it clearer.

Comment, Ref. 2: **In the discussion of Figure 14 (Section 3.4, lines 8-20), please clarify whether the decreases and increases discussed and the vector lengths shown in Figure 14 are absolute differences or normalized differences (eg. Percentage change)?**

Markup document: Page 10, lines 4 - 5
The values and vector lengths shown are absolute differences. These values are all less than 1. You can think of them as scaling factors that scale down the optimal productivity based on nutrient and light limitation. This additional explanation is included in the text.

Comment, Ref. 2: **Equation 10 is not clear. Please explain C. Is it a factor multiplying only (nlim+llim)3?**
Markup document: Page 10, line 24

Yes, C is a constant multiplying only the first term. We added the phrase "where C is a constant" in the text below the equation. Reducing equation 9 gives

$$B = P^*(\frac{P_0^C}{\lambda_0}) \cdot ((\frac{P_0^C}{\lambda_0})^2 (nlim \cdot llim)^3 + (nlim \cdot llim)).$$

C in the manuscript equals $(\frac{P_0^C}{\lambda_0})^2$, a constant.

Comment, Ref. 2: **In Introduction, the paragraph starting in line 25 explains how CDM abundance is not a local property of the seawater (as maybe chl is) because it is determined to a large degree by riverine outflow or continental runoff which in turn is determined by conditions on land and has large seasonal cycle, particularly at mid and high latitudes. Annual means, as being used in this study, are therefore not well representing the actual change of CDM in these regions.**

Markup document: Page 11, line 26 to Page 12, line 2
We struggled with the choice to use an annual average instead of a monthly climatology, for the reasons the reviewer mentioned. The downside of using a monthly climatology is the reduced spatial coverage in higher latitudes. We thought it was most important to minimize the total area where satellite data was missing. We agree that our use of an annual average does not capture the seasonal variability of CDM in the ocean and state this explicitly in line 28. We edited our discussion of this topic and included a statement about our use of annual mean data.

Comment, Ref. 2: **Section 2.2 line 16: with regards to seasonal variability, please see earlier comment about riverine and coastal runoff which are largely responsible for CDOM distributions there. Annual means will underestimate the effect in light attenuation. Please discuss this point.**

Markup document: Page 11, line 26 to Page 12, line 2
See response to comment above. We will included a discussion of how the annual average underestimates CDOM during certain months of the year in areas that are affected by coastal runoff.

Markup document: Page 22, lines 11-15
This issue is also mentioned in the Conclusion section in the discussion of simplifications in this study.

Comment, Ref. 1: **Pg 3915, Line 3. It is simply stated that the comparison is for "average results for the final 100 years of the model runs". Would be nice to know how that time period came about and how sensitive the results are to the time average.**

Markup document: Page 12, lines 13 - 16
One hundred years is long enough to average over most interannual variability in the model. For example, 20 years is not long enough because of the influence of El Nino decadal variability. We analyze the final 100 years of the model runs to eliminate the influence from spinup, which we consider to be the period of time it takes for a distinct signal to develop. For the model experiments discussed in this paper the spinup time is less than 50 years. This information is now in the

manuscript.

Comment, Ref. 2: **Section 3.2, line 23: "Biological productivity moves up the column. . ." This is not an accurate expression. BP does not "move up" the column, rather it increases near the surface and decreases below. Please correct this expression here and elsewhere it appears.**

Markup document: Page 13, line 12
The wording was changed as suggested.

Markup document: Page 16, lines 15-16
The wording was changed as suggested.

Comment, Ref. 2: **Section 3.2, line 27: particulate matter is consumed in the water column" do the authors mean "particulate matter is remineralized"? It seems to me that would be the most appropriate notion here.**

Markup document: Page 13, line 15
We changed the word *consumed* to *remineralized*.

Comment, Ref. 2: **Why is Figure 10 mentioned before Figure 9. Please order Figures as they appear in the text.**

We checked to make sure the figures are mentioned in order in the text.

Comment, Ref. 2: **Section 3.4, paragraph starting with line 3. I am not clear, as to what causes the changes in biomes. The authors state that the biomes are computed based on winter mixed layer depth, vertical velocities and ice extent, following Sarmiento et al (2004). All these are physical model changes, which imply that SST changes when chl changes. If that is the case, I would like to see a model validation of SST in the "chl&cdm"run and the "chl only" run.**

Markup document: Page 15, line 17 to Page 16, line 2 & Pages 40 - 41, Figs. 12 & 13
The physical and biogeochemical models are coupled. Changes in chlorophyll concentration can change SST according to our model configuration. This is why the biome areas are different between the two model runs. Further clarification and model validation are now included in the text.

Markup document: Pages 40 - 41, Figs. 12 & 13
The SST contour plot in Fig. 12 shows modeled (chl&CDM) minus observed using NOAA_OI_SST_V2 data provided by the NOAA/OAR/ESRL PSD, Boulder, Colorado, USA, from their Web site at http://www.esrl.noaa.gov/psd/ (Reynolds, 2002). The RMS error between annually averaged modeled and observed SST is 1.5°C. Additional validation details for the physical ocean model can be found in Galbraith et al (2011). Chl-only minus observed is not shown because the differences are qualitatively similar to those shown in Fig. 12. The differences in SST between the two models runs are small. See Fig. 13.

Markup document: Page 25, lines 1 - 2
We added a bibliography entry for the SST observational data field.

Comment, Ref. 1: **Figure 12 The 40% decrease in irradiance at 145 m depth suggests a significant change. However, in absolute terms, back of the envelope calculations following Morel (1988) suggest that for a relatively large noontime surface irradiance value (1000 W/m^2) and a modest upper ocean chlorophyll concentration (0.1 mg/m^3), the net irradiance at 145 m depth is $<$0.01 W/m^2, and most likely insignificant. Curves (probably on a log scale) should be added to Figure 12 showing absolute changes.**

Markup document: Page 16, line 23 & Page 43, Fig. 15
We changed the the figure to show the absolute changes in irradiance at depth, so as to more accurately portray the differences in irradiance. In Figure 15, the irradiance plot is shown with semilog axes. Difference at 196m is zero. We removed the word "relative" on page 16.

Comment, Ref. 2: **Figures 13 and 14 are a very nice representation of the changes in the 2dimensional limitations space.**

We thank the reviewer for this comment. No associated changes made.

Comment, Ref. 1: **Pg 3915, Line 10. An artifact of the "new" parameterization is a decrease in attenuation due to the Chl component alone. So, in regions with little CDOM, the "new" parameterization that adds (CDOM) attenuation can actually result in decreased (overall) attenuation. The manuscript would benefit by an additional sentence or two commenting on this result. For example, is it an unintended consequence of the "new" curve (surface) fit? Does it make physical sense?**

Markup document: Page 20, lines 12 - 21 & Page 47, Fig. 19
The reviewer is commenting on the observation that the parameterization used for the diffuse attenuation coefficient used in previous studies (equation 3) and the parameterization presented in this paper (equation 5) exhibit a different functional dependence on chl. The chl coefficient and exponent in equation 5 is smaller than the chl coefficient in equation 3. This was an expected result since the parameterization used in previous studies combined the attenuation by chl and CDM into a single chl term. Separating the contribution of those two aquatic constituents would give less weight to the chl term. The reviewer correctly conjectured that there are regions with little attenuation by CDM where the model run with the parameterization as presented in this paper (equation 5) results in decreased surface attenuation compared to a model run using equation 3. These results are shown in Figure 19. Attenuation depth increased by an average of 0.9m in locations where the difference in attenuation depth was positive (chl&CDM minus model run using equation 3). This information was added to the manuscript.

Comment, Ref. 2: **Section 3.2. It is a very good idea that the authors chose to disentangle chl from CDM in their runs and compare equation (5), i.e. run "chl&CDM", with equation (5) without CDM "chl only run". However, it would be informative to see the comparison of equation (5) with results from the model when Equation (4) was used. The reason is that, as**

the authors state in Section 2.2, lines 19-23 and show in Figure 4, the earlier parameterization produced higher distributions of chl compared to observations, and I wonder whether the new parameterization will further deteriorate the results. Of course, the improvement of Equation (5) is that it includes a missing process, but we still want to know what the authors think are the major sources of model error are then.

Markup document: Page 20, lines 7 - 25 & Page 47, Fig. 19
In response to this comment we swapped sections 3.3 and 3.4 and added the differences in the model runs using the old and new parameterization. The new section 3.4 is titled "Coastal Regions and Model Error". We added global trends in nutrients, biomass and chlorophyll, as well as Figure 19.

Comment, Ref. 2: **Section 3.3, lines 10-13: here the authors do compare the run including Equation (5) with the run including Equation (4), but only for coastal ocean. Would it be possible to see the same comparison for the global trends? This is also my point (10) above.**

Markup document: Page 20, lines 9 - 12
Global trends were added to the manuscript.

Comment, Ref. 1: **Pg 3921, Line 20. The manuscript states that impacts due to "altering the visible light field" are investigated. While this is technically correct, it seems that altering "attenuation of the in-water light field" is a more accurate description. The former can suggest the incident light field is altered, and that is not the case.**

Markup document: Page 21, line 2
We changed the wording exactly as suggested.

Comment, Ref. 2: **Section 4, Conclusions, line 27: Please replace the expression "movement of biological productivity higher up the water column" with the more appropriate "increase of biological productivity in the upper water column and decrease below" or similar.**

Markup document: Page 21, lines 11 - 12
We changed the wording as suggested.

Comment, Ref. 2: **How do adg/chl values from MODIS compare with the NOMAD values that were used in obtaining Equation (5)?**

We did not matchup in situ measurements with satellite-derived data products because we consider this to be outside the scope of our study. We refer readers to publications pertaining to the performance of the GSM $a_{dg}(443)$ product for this type of analysis. We do not utilize the chlorophyll data product from MODIS for our model runs, and thus find a comparison of in situ vs. satellite estimates irrelevant to our study. Chlorophyll concentration is predicted by the biogeochemical model. We did not think this comment warranted any change to the manuscript.

Comment, Ref. 2: **Please enlarge the fonts on all figure axes, legends and contour labels as**

they are hard to read.

We enlarged fonts on axes, legends and contour labels for the following figures: 5, 6, 7, 8, 9, 14, 19.

Comment, Ref. 2: **Overall, very few typing errors exist, which a word processing software should easily capture.**

No associated changes were made.

3 Response to Technical Corrections

Comment, Ref. 1: **Pg 3908 line 20. Text indicates "studies", but then goes on to mention only a single study (Gnanadesikan and Anderson 2009).**

Markup document: Page 4, line 30 to Page 5, line 1
We changed the language of this sentence to apply to findings in both Gnanadesikan and Anderson (2009) and Manizza et al (2005).

4 Additional Corrections

Markup document: Page 6, lines 15-26
We added to our literature review.

Markup document: Page 23, lines 17-19
We included a reference to a recently published relevant study.

Markup document: Page 24, lines 6-8
We referenced more relevant work by Gregg and Casey.

Manuscript prepared for Biogeosciences Discuss.
with version 2014/07/29 7.12 Copernicus papers of the LaTeX class copernicus.cls.
Date: 15 June 2015

~~A new parameterization for surface ocean light attenuation in Earth System Models: assessing~~ Quantifying the biological impact of surface ocean light ~~absorption~~ attenuation by colored detrital ~~material~~matter in an ESM using a new optical parameterization

G. E. Kim, M.-A. Pradal, and A. Gnanadesikan

Department of Earth and Planetary Sciences, 301 Olin Hall, 3400 N. Charles Street, Baltimore, MD 21218, USA

Correspondence to: G. E. Kim (gracekim@jhu.edu)

Abstract

Light ~~limitation can affect the distribution of biota and nutrients in the ocean. Light absorption~~ attenuation by colored detrital material (CDM) was included in a fully coupled Earth System Model~~using a new~~ . This study presents a modified parameterization for shortwave attenuation~~. Two model runs~~ , which is an empirical relationship between 244 concurrent measurements of the diffuse attenuation coefficient for downwelling irradiance, chlorophyll concentration and light absorption by CDM. Two ESM model runs using this parameterization were conducted, with and without light ~~attenuation~~ absorption by CDM. ~~In a global average sense, greater~~ The light absorption coefficient for CDM was prescribed as the average of annual composite MODIS Aqua satellite data from 2002 to 2013. Comparing results from the two model runs show that changes in light limitation associated with ~~CDM increased surface~~ the inclusion of CDM decoupled trends between surface biomass and nutrients. Increases in surface biomass were expected to accompany greater nutrient uptake and therefore diminish surface nutrients. Instead, surface chlorophyll, biomass and nutrients increased together. These changes can be attributed to the ~~movement of biological productivity higher up the water column, which increased surface chlorophyll and biomass while simultaneously decreasing total biomass. Meanwhile, the reduction in biomass resulted in greater nutrient availability throughout the water column~~different impact of light limitation on surface productivity versus total productivity. Chlorophyll and biomass increased near the surface but decreased at greater depths when CDM was included. The net effect over the euphotic zone was less total biomass leading to higher nutrient concentrations. Similar results were found ~~on a regional scale in an~~ in a regional analysis of the oceans by biome investigating the spatial variability of response to changes in light limitation using a single parameterization for the surface ocean. In coastal regions, surface chlorophyll increased by 35 % while total integrated phytoplankton biomass diminished by 18 %. The largest relative increases in modeled surface chlorophyll and biomass in the open ocean were found in the equatorial biomes, while largest decreases in depth-integrated biomass and chlorophyll were found in the subpolar and polar biomes. This mismatch of

surface and subsurface trends and their regional dependence was analyzed by comparing the competing factors of diminished light availability and increased nutrient availability on phytoplankton growth in the upper 200 m. ~~Overall, increases in surface biomass were expected to accompany greater nutrient uptake and therefore diminish surface nutrients, but changes in light limitation decoupled trends between these two variables.~~ Understanding changes in biological productivity requires both surface and depth-resolved information. Surface trends may be minimal or of the opposite sign to depth-integrated amounts, depending on the vertical structure of phytoplankton abundance.

1 Introduction

The attenuation of shortwave solar radiation in the surface ocean exerts a primary control on ocean biology, since light is necessary for photosynthesis by phytoplankton. The decay of incident surface irradiance $I_{\mathrm{d}}(0,\lambda)$ with increasing depth z in the water column can be approximated as an exponential function:

$$I_{\mathrm{d}}(z,\lambda) = I_{\mathrm{d}}(0,\lambda)\exp\left(-\int_0^z k_{\mathrm{d}}(z',\lambda)\mathrm{d}z'\right), \tag{1}$$

where k_{d} (units of m^{-1}) is the spectral attenuation coefficient for downwelling irradiance. The reciprocal of k_{d} is the first e-folding depth of the incident light on the surface of the ocean, an intuitive length scale for the well-lit surface ocean. Variations in shortwave attenuation have been related to measured quantities of constituents in the aquatic medium, such as concentrations of the phytoplankton pigment ~~concentration~~ chlorophyll a. Morel (1988) observed increasing k_{d} with increasing chlorophyll a pigment concentration in 176 concurrent in situ measurements, excluding stations where light attenuation was dominated by "yellow substance" or turbidity. These measurements were used to develop a function that relates k_{d} to chlorophyll a concentration of the form:

$$k_{\mathrm{d}}(\lambda) = k_{\mathrm{w}}(\lambda) + \chi(\lambda)[\mathrm{chl}]^{e(\lambda)}, \tag{2}$$

where $k_w(\lambda)$ is the attenuation by pure seawater, [chl] is the chlorophyll a concentration and $\chi(\lambda)$ and $e(\lambda)$ are the wavelength-dependent coefficient and exponent. This parameterization implicitly includes the light attenuation of all other aquatic constituents presumed to be directly in proportion ~~to~~ with chlorophyll concentration. Ohlmann and Siegel (2000) used a radiative transfer numerical model to develop an extended parameterization for k_d which depended on chlorophyll concentration, cloudiness and solar zenith angle to include the effects of varying physical conditions over ocean waters. Among these four variables, chlorophyll concentration was found to have the largest influence on reducing solar transmission below 1 m.

These initial parameterizations have been adapted for use in Ocean General Circulation Models (OGCMs) and Earth System Models (ESMs) to study the influence of spatially varying light attenuation associated with varying concentrations of phytoplankton pigments in the ocean. Although numerous model experiments of this type ~~were~~ have been conducted, we mostly limit our introductory material to studies that utilized versions of the parameterization shown in Eq. (2). These studies examined the effects of applying a spatially varying k_d calculated from annual mean chlorophyll data, estimated by ocean color satellites, compared to the base case of a constant attenuation depth. Murtugudde et al. (2002) employed the Morel parameterization (Eq. 2) spectrally averaged over visible wavelengths, from 400 to 700 nm, to calculate $k_d(\text{vis})$ ~~with~~ using chlorophyll a concentration estimates from the ~~ocean color satellite~~ Coastal Zone Color Scanner (CZCS). Spatially varying the attenuation depth improved the OGCM SST simulation in the Pacific cold tongue and during ENSO events and in the Atlantic near river outflows. Subsequent studies employed an optics model that separately attenuated visible light in two bands of equal energy, nominally the "blue-green", $k_d(\text{bg})$, and "red" bands, $k_d(r)$, as specified in (Manizza et al., 2005):

$$k_d(\text{bg}) = 0.0232 + 0.074 \cdot [\text{chl}]^{0.674} \quad (3)$$

$$k_d(r) = 0.225 + 0.037 \cdot [\text{chl}]^{0.629}. \quad (4)$$

Studies that applied this k_d parameterization in ~~fully coupled~~ ESMs were uniquely able to assess how changes in oceanic shortwave absorption can affect atmospheric and oceanic

circulation via changes in ~~SST~~sea surface temperature (SST). Gnanadesikan and Anderson (2009) observed changes in strength of the Hadley and Walker circulations when applying a spatially-varying k_d using chlorophyll concentration from the SeaWiFS (Sea-viewing Wide Field-of-view Sensor) ocean color satellite relative to a clear ocean with no chlorophyll. Alternatively, Manizza et al. (2005) applied this parameterization to an OGCM with a biogeochemical model to calculate k_d using modeled chlorophyll concentration instead of surface chlorophyll estimates from satellite. The main advantage of the latter model configuration is that phytoplankton can respond to changes in environmental variables. They found that adding phytoplankton amplified the seasonal cycles of SST, mixed layer depth and sea-ice cover, which in turn created environmental conditions that were favorable to additional phytoplankton growth.

~~Although variations~~ Variations in light attenuation in ESMs were previously attributed to ~~phytoplankton pigment only, other~~ chlorophyll and implicitly to aquatic constituents assumed to vary in proportion to chlorophyll. Other optically significant aquatic constituents can now be explicitly incorporated into models. This paper is concerned with the omission of colored detrital material (CDM) in approximations of light decay in the current generation of ESMs. CDM consists of chromophoric dissolved organic matter (CDOM) and non-algal detrital particles (NAP). It is operationally defined by its spectrally-dependent absorption coefficient of light, a_{dg} (units of m^{-1}), which represents the fraction of incident power that is absorbed by detrital matter in a water sample over a given pathlength. The absorption coefficient is given the subscript "dg" to represent the sum of the two component absorption coefficients; (1) non-algal detrital particles, a_{NAP}, and (2) light-absorbing dissolved organic matter which passes through a 0.2–0.4 µm filter, a_{CDOM}, (called *gelbstoff* by early researchers in optical oceanography, hence the "g" in "dg"): $a_{dg} = a_{NAP} + a_{CDOM}$. Measurements suggest CDOM accounts for a large fraction of non-water absorption in the open ocean ~~, especially~~ in the UV and blue wavelengths (Siegel et al., 2005; Nelson and Siegel, 2013). The attenuation of light by this strongly absorbing component should be included in Earth System Models. Although light absorption by NAP is a small fraction of CDM absorption (see Fig. 1), the sum

of NAP and CDOM is considered because existing satellite algorithms cannot separate the contribution of each component.

~~Moreover, parameterizing~~ Parameterizing k_d using Eq. (2) relies on the validity of the bio-optical assumption, which states that all light-attenuating constituents covary with chlorophyll concentration. Yet processes that influence CDM abundance, such as freshwater delivery of terrestrial organic matter and photobleaching, can behave independently of chlorophyll a concentration, rendering the bio-optical assumption inappropriate for some aquatic environments. In an analysis of satellite ocean color data products, Siegel et al. (2005) show correlation between chlorophyll and CDM distributions in subtropical gyres and upwelling regions. These variables are found to be independent in subarctic gyres, the Southern Ocean and coastal regions influenced by land processes such as coastal and river runoff. In this paper, we will consider the impact of decoupling the optical influence of chlorophyll a and CDM in Earth System Models. **?** ~~previously developed a more optically complex model for surface ocean irradiance based on light~~

Recent studies have incorporated the optical properties of additional in-water constituents into global ocean biogeochemical simulations. Gregg and Casey (2007) calculate in-water radiative properties using the absorption and scattering of ~~aquatic constituents. However, this study was primarily concerned with accurately modeling surface irradiance and photosynthetically available radiation for comparison with in situ and satellite data. The current paper is concerned with using an Earth System model~~ water, phytoplankton groups and CDOM in a coupled ocean circulation-biogeochemical-radiative model. Dutkiewicz et al. (2015) assess the bio-optical feedbacks of detrital matter, CDOM and phytoplankton by explicitly representing these components in their ocean biogeochemistry-ecosystem model. In this paper we use a fully coupled Earth System Model to better understand how changes in light ~~will~~ attenuation from including CDM affect ocean ecosystems.

In Sect. 2, we introduce the global ocean color dataset for the absorption coefficient of detritus and CDOM, and discuss its incorporation into the GFDL CM2Mc ESM with BLING biogeochemistry model. This is accomplished using a newly developed parameterization

for $k_d(\lambda)$, which aims to represent light attenuation by chlorophyll a and CDM as independently varying phenomena. (For the remainder of this paper, we will refer to chlorophyll a concentration simply as chlorophyll.) Section 3 details the model runs and the results, with a focus on how changes in light affect chlorophyll, biomass and nutrient concentrations. The paper concludes with Sect. 4, discussing the implications of our findings and suggestions for future work.

2 Methodology

2.1 Light penetration parameterization

A new k_d parameterization was developed for implementation in the GFDL CM2Mc ESM (Galbraith et al., 2011) with BLING ocean biogeochemistry (Galbraith et al., 2010). In its current configuration, the CM2Mc-BLING system uses the Manizza et al. (2005) optics model and k_d parameterization as shown in Eqs. (3) and (4). The new parameterization was developed from this optics model, revising the $k_d(\text{bg})$ parameterization only (Eq. 3). The $k_d(r)$ parameterization was unchanged because light absorption by CDOM is very small compared to absorption by seawater and chlorophyll in the red wavelengths. This is apparent by examination of the spectral shapes of these constituents in ~~red wavelengths is much smaller than in the blue-green wavelengths which can be seen from the spectral shape of a_{dg} in~~ Fig. 1. The new $k_d(\text{bg})$ parameterization incorporates the absorption coefficient of detritus and CDOM at wavelength 443 nm, $a_{dg}(443)$, because ~~field measurements of a_{dg} are available at this wavelength. In addition,~~ existing satellite data products of a_{dg} are readily available for this wavelength only.

In the new parameterization, the dependence of $k_d(\text{bg})$ on both chlorophyll concentration and $a_{dg}(443)$ is the best fit function between concurrent in situ measurements of these variables from the NASA bio-Optical Marine Algorithm Dataset (NOMAD) (Werdell and Bailey, 2005). Measurements of k_d from 400 to 530 nm were energy-weighted and averaged to get a single value for the attenuation coefficient in the blue-green wavelengths. There

were 244 concurrent measurements of $k_d(\text{bg})$, chlorophyll concentration and $a_{dg}(443)$ from the NOMAD dataset, representing both coastal and open ocean waters. The locations of these measurements are shown in Fig. 2. The stations were arbitrarily grouped by region and color coded: (1) western Atlantic, northern cluster in black; (2) western Atlantic, Amazon river outflow and offshore stations in green; (3) Antarctic peninsula in orange; (4) Southern Ocean in blue; (5) western Pacific in magenta; (6) stations across the Pacific ocean in red and (7) eastern Pacific in cyan. We found poor correlation between chlorophyll concentration and $a_{dg}(443)$ at these stations, as shown in Fig. 3. The best fit surface for ~~these three variables~~ $k_d(\text{bg})$, chlorophyll concentration and $a_{dg}(443)$ was found using a least-squares polynomial regression model using the Levenberg-Marquardt algorithm, resulting in the following parameterization:

$$k_d(\text{bg}) = 0.0232 + 0.0513 \cdot [\text{chl}]^{0.668} + 0.710 \cdot a_{dg}(443)^{1.13}. \quad (5)$$

We conducted a sensitivity analysis to assess the importance of each region for obtaining the parameters by removing one regional cluster from the regression fitting at a time. The parameters were mostly stable. The exponent to the chlorophyll term was the only term that changed by an amount that well exceeded the fitting uncertainty, increasing by 0.23 when the eastern Pacific stations were omitted.

Figure 4 panels (a) and (b) show an improved fit between modeled and measured $k_d(\text{bg})$ when using Eq. (5). Equation (5) is qualitatively different from the previous parameterization, Eq. (3), in several ways. The attenuation coefficient is less dependent on chlorophyll concentration, with a smaller coefficient and exponent on the chlorophyll term in Eq. (5) compared to Eq. (3). Meanwhile, the additional $a_{dg}(443)$ term makes the water more opaque in locations where CDM and chlorophyll concentration are not well correlated, such as coastal zones that are strongly influenced by the terrestrial delivery of CDOM. The k_d dependence on $a_{dg}(443)$ is superlinear, which at first glance seems to suggest an unexpectedly strong dependence on CDOM and detrital particles. We suggest this superlinear relationship is justified because the parameterization is fitting for spatial variations in CDOM quality and quantity. Measurements of ~~the~~ a_{dg} across the ultraviolet to visible spectrum suggest the

spectral dependence of light absorption by CDOM is regionally specific (Nelson and Siegel, 2013).

2.2 Implementation in ESM

This parameterization was implemented in the GFDL CM2Mc ESM, a coarse resolution coupled global climate model with land, ice, atmosphere and ocean components (Galbraith et al., 2011). The Modular Ocean Model version 4p1 code is used to simulate the ocean. The model has a varying horizontal resolution from ~~0.6 to 3~~1.01 to 3.39° and 28 vertical levels of increasing thickness with depth. Ocean biogeochemistry is represented by the Biogeochemistry with Light, Iron, Nutrients and Gases model (BLING), which is embedded in the ocean component of the physical model (Galbraith et al., 2010). The coupling between the biogeochemical model and physical model allows changes in chlorophyll concentration to produce changes in shortwave radiation absorption and vice versa. Since the same optical model is used for calculating light attenuation for physics and biology in our ESM configuration, the same attenuation depth is used in simulating physical processes and biological productivity. For example, the optical model calculates light attenuation using model-derived chlorophyll concentration. Increases in chlorophyll concentration reduce the attenuation depth, reducing total light available for biological processes such as photosynthesis and physical processes such as the total shortwave heating of the ocean. However, by utilizing one optical parameterization for the entire ocean, regionally-specific variations of the functional dependence of light attenuation on chlorophyll and CDM are not represented in this model setup.

In the BLING biogeochemical model, phytoplankton growth rate is calculated implicitly as a function of temperature, macronutrient concentration, iron concentration and light.

$$\mu = P_0^{\mathrm{C}} \times \exp(kT) \times \mathrm{nlim} \times \mathrm{llim} \tag{6}$$

where μ is a carbon-specific growth rate, P_0^{C} is a maximum growth rate at 0 °C, $\exp(kT)$ is a temperature-dependent term based on Eppley (1972), $\mathrm{nlim} = \min(\mathrm{Fe_D}, \frac{\mathrm{PO_4}}{k_{\mathrm{PO_4}}+\mathrm{PO_4}})$ is

a nutrient limitation term following a Liebig's law of the minimum and $\text{llim} = (1 - \exp(\frac{-I}{I_k}))$ is a light limitation term. These nutrient and light limitation factors, nlim and llim, represent the extent to which the optimal photosynthetic growth rate is scaled down by nutrient and light availability. Mathematically, nlim and llim have values between 0 and 1 that scale down the optimal photosynthetic rate as they are multiplied by P_0^C. Furthermore, these are the only two variables that determine biomass in the BLING model. Total biomass is a sum of large and small phytoplankton groups, which are related to growth rate μ by the following equation

$$B = B_{\text{large}} + B_{\text{small}} = P^* \left(\left(\frac{\mu}{\lambda} \right)^3 + \left(\frac{\mu}{\lambda} \right) \right) \tag{7}$$

where B is biomass, P^* is a scale factor for phytoplankton concentration and λ is a temperature-dependent mortality rate

$$\lambda = \lambda_0 \times \exp(kT). \tag{8}$$

Substituting Eqs. (6) and (8) for μ and λ into Eq. (7), gives us

$$B = P^* \left(\left(\frac{P_0^C \times \exp(kT) \times \text{nlim} \times \text{llim}}{\lambda_0 \times \exp(kT)} \right)^3 + \left(\frac{P_0^C \times \exp(kT) \times \text{nlim} \times \text{llim}}{\lambda_0 \times \exp(kT)} \right) \right) \tag{9}$$

Following Dunne et al. (2005), the temperature dependence of the mortality rate is set identical to that of the growth rate such that the $\exp(kT)$ term in both μ and λ expressions are identical, Eq. (9) reduces to the following relationship between biomass, nutrient limitation and light limitation

$$B \propto (C(\text{nlim} \times \text{llim})^3 + (\text{nlim} \times \text{llim})). \tag{10}$$

where C is a constant. Dunne et al. (2005) found that such a formulation was able to reproduce the observed phytoplankton size structure ~~in~~ across 40 ~~samples~~sites. This allows us

to separately evaluate the contributions of nutrient and light limitation to changes in biomass in our biogeochemical model. This relationship will be utilized in the Results section of our paper.

Chlorophyll concentration is calculated from biomass using a varying chl : C ratio to account for photoadaptation. Large scale patterns and features of chlorophyll concentration are qualitatively represented, with lower chlorophyll concentration in the gyres and higher concentrations in mid- to high-northern latitudes and equatorial upwelling zones (see Fig. 5). In general, the annual average modeled chlorophyll exceeds the satellite observed chlorophyll concentration in the open ocean. The seasonal cycle is also well-represented, but with a northern latitude spring bloom onset earlier than appears in satellite data. There is good spatial agreement between the modeled and observed spatial distribution of ~~macronutrient~~macronutrients, which is shown in Fig. 6. BLING only models phosphate concentration, which is comparable to an "average macronutrient" that represents the average concentrations of phosphate and nitrate scaled to phosphate by the N : P Redfield ratio, $\frac{1}{2}(\mathrm{PO_4} + \frac{\mathrm{NO_3}}{16})$ (Galbraith et al., 2010). The error in chlorophyll and nutrient concentrations in this implementation of BLING are worse than in Galbraith et al. (2010) because the model parameters were originally tuned to a data-driven ocean model. As a result, errors that appear in the physical circulation will also appear in the biological solution.

The ocean optical model receives incoming shortwave radiation from the atmospheric component. Visible light is divided and then averaged into two spectral bands, blue-green and red, which ~~is~~ are then attenuated by $k_\mathrm{d}(\mathrm{bg})$ and $k_\mathrm{d}(r)$ respectively. In its previous configuration, BLING calculated $k_\mathrm{d}(\mathrm{bg})$ as a function of chlorophyll concentration as shown in Eq. (3). For this study, $k_\mathrm{d}(\mathrm{bg})$ is calculated using Eq. (5) with model-predicted chlorophyll concentration and fixed $a_{\mathrm{dg}}(443)$ from satellite climatology. The $a_{\mathrm{dg}}(443)$ dataset used in this study is the average of the 2002 to 2013 Aqua MODIS GSM $a_{\mathrm{dg}}(443)$ Level 3 annual composites from http://oceancolor.gsfc.nasa.gov. Annual average data was used instead of monthly data to maximize the number of grid cells with unimpeded satellite observations. Consequently the seasonal variability of CDM is not represented in our model runs. ~~The~~ By fixing $a_{\mathrm{dg}}(443)$ as a constant value throughout the year, light absorption by CDM is

underestimated in months where riverine and coastal runoff deliver additional CDOM to the ocean. The averaged satellite data was re-gridded to the ocean model's spatial resolution and missing values were filled in by equal weight averaging over the pixel's 8 neighbors using Ferret, a data visualization and analysis tool for gridded datasets (see Fig. 7). ~~Annual average data was used instead of monthly data to maximize the number of grid cells with unimpeded satellite observations.~~ Satellite-estimated values of surface $a_{\mathrm{dg}}(443)$ were held constant with increasing depth.

3 Model runs: setup, results and discussion

3.1 Model setup

The GFDL CM2Mc ESM with BLING ocean biogeochemistry was spun up for 1500 years with the Manizza et al. (2005) ocean optics model, allowing dynamical processes to reach equilibrium. New model runs were initialized from this spun up state and were completed for an additional 300 years. ~~The data analyzed~~ We analyzed the final 100 years of the model runs to average over interannual variability and to eliminate the influence from spinup, which we consider to be the period of time it takes for a distinct signal to develop. For the model experiments discussed in this paper the spinup time was less than 50 years. The data presented in this section are average results from the final 100 years of the two model runs: the (1) "chl&CDM" run utilizes the full $k_{\mathrm{d}}(\mathrm{bg})$ parameterization, Eq. (5), while the (2) "chl-only" run calculates light attenuation with the chlorophyll-dependent term only: $k_{\mathrm{d}}(\mathrm{bg}) = 0.0232 + 0.0513 \cdot [\mathrm{chl}]^{0.668}$. The difference between ~~these~~ the two model runs (chl&CDM minus chl-only) shows the impact of added shortwave attenuation by CDM. For the remainder of this paper we will refer to $k_{\mathrm{d}}(\mathrm{bg})$ as k_{d} for simplicity.

3.2 Model results: global trends

Adding CDM to the k_{d} parameterization shoaled the attenuation depth (k_{d}^{-1}, in m) in most places. This change in the light field was accompanied by a globally integrated 10 % in-

crease in surface macronutrients, 11 % increase in surface biomass and 16 % increase in surface chlorophyll. These changes reflect the total ~~integrated~~ value from the surface grid ~~box, which represents~~ boxes, which represent the uppermost 10 m. At first glance, this result was puzzling since increases in chlorophyll and biomass are generally associated with increased nutrient consumption, which is usually indicated by decreased nutrient concentration. Instead, all three variables increased together. The spatial distributions of surface changes in macronutrients, chlorophyll concentration and biomass are shown in Fig. 8.

In order to understand these surface changes, it is necessary to evaluate changes in the biomass depth profile. Globally averaged biomass and particulate organic carbon (POC) export flux in the chl&CDM run are higher near the surface but diminished at depth, as shown in Fig. 9. ~~Biological productivity moves up in the water column, which explains the increase in surfacechlorophyll. Below~~ Chlorophyll increases at the surface, but below 25 m ~~,~~ there is less biological productivity in the chl&CDM run. The depth-integrated result is a 9 % decrease in total biomass. Furthermore, since biological productivity is occurring closer to the surface, particulate matter is ~~consumed~~ remineralized in the water column and less is exported into the deep ocean. This can be seen in Fig. 9b. The cumulative effect is a 7 % decrease in POC flux at 200 m.

This upward shift in the vertical distribution of biomass was accompanied by increased macronutrients at all depths. Here, we will consider the distribution of macronutrients in the top 200 m as a measure of the biological activity in the mixed layer according to the biological pump efficiency, E_{bp}, defined in Sarmiento and Gruber (2006) as: $E_{\text{bp}} = \frac{C_{\text{deep}} - C_{\text{surface}}}{C_{\text{deep}}}$. This metric provides a indication of the extent to which phytoplankton are able to draw down nutrients delivered to the surface from the deep ocean. Here, C_{surface} is the integrated nutrient concentration between 0 and 100 m and C_{deep} is the integrated nutrient concentration between 100 and 200 m. The difference in E_{bp} between the two model runs shows a widespread decrease in biological pump efficiency when CDM is included (see Fig. 10). In a global average sense, increased light limitation by CDM diminishes total biomass, leaving excess nutrients in the water column. Nutrients are more abundant and phytoplankton are less effective at utilizing them when the ocean is more light limited. The spatial correlation

between the difference in E_{bp} and a_{dg} is -0.26, indicating a general negative relationship between the two variables. However, regions of greatest light absorption by CDM are not always the same regions of greatest decrease in E_{bp} for reasons that will be discussed in the following subsections.

3.3 ~~Coastal regions~~Ocean biomes

The ~~distribution of light absorption by CDM in Fig. 7 and diminished attenuation depth in Fig. 8 suggest the addition of CDM to the optical model would have a significant impact on ocean productivity in coastal regions. For the following analysis , coastal regions were defined as grid cells adjacent to land.~~

~~In coastal regions, surface nutrients increased by 16 , surface biomass by 22 and surface chlorophyll by 35 . Depth-integrated trends were of the opposite sign compared to surface trends. Total biomass decreased by 18 and total chlorophyll decreased by 17 when CDM was included. The largest percentage changes in integrated biomass were found in the equatorial latitudes, which experienced up to 38 drops in coastal biomass. High northern latitudes north of 60 N experienced 17–36 decreases in coastal biomass. Relative changes in depth-integrated coastal biomass are shown by latitude in Fig. 18.~~

~~These results are reported with the understanding that the coastal circulation is likely to be poorly resolved in our coarse model. Nonetheless, they highlight the potential impact of including the optical impact of CDM in coastal regions. The results shown in this paper compare the "chl&CDM" and "chl-only" model runs. A comparison of the output of the "chl&CDM" model run and a model run with the original k_d parameterization, Eq. (3), show similar trends. In coastal regions, surface nutrients increased by 1 , surface biomass by 3 and surface chlorophyll by 6 , while depth-integrated biomass and chlorophyll decreased by 9 compared to the "chl&CDM" model run. It will be increasingly important for models to include the optical impact of CDM to avoid the potential error of misrepresenting light attenuation as models with finer grid resolution are developed, especially in coastal regions.~~

3.4 ~~Open ocean biomes~~

~~The analysis in this~~ analysis in this section will address changes in nutrient concentration and biological productivity by ocean biome. Following Sarmiento et al. (2004), we use average vertical velocity, maximum wintertime mixed layer depth and sea ice cover to define six biomes that are differentiated based on physical circulation features. They are: (1) equatorially influenced, between 5° S and 5° N, divided into upwelling and downwelling regions, (2) marginal sea ice zones that are covered by sea ice at least once during the year, (3) permanently stratified subtropical biomes where downwelling occurs and maximum mixed layer depth is ≤ 150 m, (4) seasonally stratified subtropical biomes where downwelling occurs and maximum mixed layer depth >150 m, (5) low-latitude upwelling regions between 35° S and 30° N, and (6) all subpolar upwelling regions north of 30° N and south of 25° S. Boundaries were determined based on circulation features from the respective model runs for consistency. See Fig. 11 for a visual representation of biome extent for the chl&CDM model run.

The largest changes in biome areal extent include a 19 % increase in the Northern Hemisphere marginal ice zone and -9 % change in the extent of the neighboring subpolar Northern Hemisphere biome, as shown in table 1. The biome area changes between the two model runs because the biological and physical models are coupled. The added light attenuation by CDM in the optical model affects both biological production and physical variables such as SST in our ESM configuration. Furthermore, the changes in chlorophyll concentration from the increased light attenuation change the attenuation depth in the physical model. The SST contour plot in Fig. 12 shows modeled (chl&CDM) minus observed using NOAA_OI_SST_V2 data provided by the NOAA/OAR/ESRL PSD, Boulder, Colorado, USA, from their web site at http://www.esrl.noaa.gov/psd/ (Reynolds, 2002). The RMS error between annually averaged modeled and observed SST is 1.5°C. Additional validation details for the physical ocean model can be found in Galbraith et al. (2011). The chl-only model run minus observed is not shown because the differences are qualitatively similar to

those shown in Fig. 12. The differences in SST between the two models runs are small, as shown in Fig. 13.

Differences in surface chlorophyll, biomass and macronutrients between the two model runs (see table 2) show the addition of CDM results in several important qualitative and regionally specific changes. For example, the greatest relative change in chlorophyll and biomass over the upper 10 m are found in equatorial and low latitude biomes, with 15–17 % increases in biomass and 21–24 % increases in chlorophyll. Meanwhile, the greatest changes in depth-integrated chlorophyll and biomass are found in high latitude regions. In the Northern Hemisphere subpolar biome, chlorophyll decreased by 14 % and biomass decreased by 15 %. Chlorophyll and biomass decreased by 9 and 10 % respectively in the Southern Hemisphere marginal ice zone. The following analysis seeks to understand this mismatch between surface and subsurface trends between biomes. In particular, why are the largest changes in surface chlorophyll near the equator and largest changes in depth-integrated chlorophyll at higher latitudes?

As shown in previous sections, phytoplankton ~~move up in the water column~~ increase at the surface and decrease below when CDM is included. The resulting vertical profile of chlorophyll is altered in different ways depending on the biome. To illustrate, we choose three representative biomes from various latitudes, for which chlorophyll profiles are shown in Fig. 14. In the equatorial upwelling and seasonally stratified biomes, the deep chlorophyll maximum is increased. In the ice NH region, where light delivery is seasonally dependent, chlorophyll is found in highest concentrations near the surface and is diminished at depth. In every biome, there is more chlorophyll near the surface but less chlorophyll beyond some depth. These changes can be attributed to a combination of diminished light availability and increased nutrient availability.

Globally averaged profiles of the ~~relative~~ difference in irradiance and macronutrient concentration are shown in Fig. 15. Over the upper 200 m, there are more nutrients and less irradiance at all depths. Referring back to Fig. 9a, there is more biomass near the surface, but diminished biomass at depth. These plots show that as we move down the water column, there is a changing balance of nutrient and light availability affecting phytoplankton

growth. The increased abundance of nutrients fuels the growth of phytoplankton near the surface. At depth, light limitation is increased to a level that results in diminished phytoplankton productivity.

We analyze the competition of light and nutrient availability on biomass using the light and nutrient limitation factors previously discussed in the Methodology section. The average light and nutrient limitation scaling factors over the surface 10 m of each open ocean biome and the coastal region for the chl-only run are shown in Fig. 16a. The coastal region was defined as grid cells adjacent to land. Consider the placement of the various biomes on this plot for the model run where light attenuation depends on chlorophyll alone. The equatorial regions are least light limited, so they lie to the right on the x axis. The marginal ice zones and subpolar regions are most light limited and lie to the left on the x axis. The Southern Hemisphere biomes are in general more nutrient limited than their Northern Hemisphere counterparts, due to modeled iron limitation. They are found lower on the y axis.

As additional light limitation is introduced by the inclusion of light absorption by CDM in the k_{d} parameterization, these markers shift. Panel b of Fig. 16 shows nlim and llim averaged over the surface 10 m for the chl&CDM model run. The displacement of ~~these points~~ each point from panel a to its new coordinates in panel b are shown in vector form in panel c. The vector begins at its coordinates from panel a, i.e. values from the chl-only run, and terminates with an "x" at the new coordinates from the chl&CDM model run. This vector indicates the change in nutrient and light limitation between the two model experiments.

The impact of these changes in light and nutrients on biomass can be seen by overlaying lines of constant biomass on these plots. Using Eq. (10), we utilize the fact that in the BLING model, biomass scales as $(C(\mathrm{nlim} \times \mathrm{llim})^3 + (\mathrm{nlim} \times \mathrm{llim}))$. In panel c, all biome vectors are pointed in the left and upward direction, indicating more nutrient availability and less light availability. The vectors cross contours of constant biomass in the direction of increasing biomass. Additional nutrient availability fuels increases in biomass in the upper 10 m of the ocean in almost every ocean biome, which is in agreement with the results reported in table 2. Panel d is similar to panel c, but with nlim, llim values averaged over the upper 200 m of the ocean. Here, the vectors are moving in a direction that crosses lines of decreasing

biomass. This is consistent with results shown in table 3. In this case, the decrease in light availability drives the decrease in biomass, despite the increase in nutrients.

The two clusters of vectors, i.e. nlim and llim averaged over (1) 0 to 10 m constituting a "euphotic regime" and (2) 0 to 200 m constituting a "subsurface regime", are shown on the same plot for comparison in Fig. 17. To first order, we think of the euphotic regime as the depth range that dominates the signal seen by satellite observations and the subsurface regime as the integrated impact over the entire ecosystem. The key difference between the two regimes is the vectors in the surface regime are crossing lines of constant biomass in the increasing biomass direction, while the vectors in the subsurface regime are crossing lines of constant biomass in the decreasing biomass direction. While there is a noticeable difference in the magnitude and angle of the vectors between these two regimes, these differences are only meaningful in the context of the vector's placement in the domain. For example, the greatest decreases in depth-integrated biomass from the inclusion of CDM were found in high latitude biomes and coastal region. This is most pronounced in the ~~costal~~ coastal region, where biomass diminished by 18 %. The corresponding magenta vector in this plot noticeably spans the greatest distance in the direction of decreasing biomass contour lines. Although the vector for the Northern Hemisphere marginal ice zone ("ice nh") is smaller, it is placed in the upper left hand corner where the contour lines are closer together. It crosses the appropriate number of lines of constant biomass to ~~indicate~~ produce the 10 % drop in biomass in this region when CDM is included. In the surface regime, the greatest increases in biomass are in the equatorial biomes. ~~The~~ While the "eq up" and "eq down" vectors are short, shown in Fig. 16c, the slope of the vector ~~indicates~~ results in sufficient positive displacement in the y direction ~~which allows for~~ to produce increasing biomass. The slope of some of the higher latitude vectors, such as the seasonal stratified biomes are more parallel to the lines of constant biomass, which accounts for the smaller changes in surface biomass.

Increases in surface chlorophyll ranged from 15 to 24 % in the equatorial, low-latitude and permanently stratified biomes. In these areas, depth-integrated biomass decreased by ≤ 6 %. These biomes comprise the cluster of vectors on the bottom right hand side of

the plot in Fig. 17. The variation in surface chlorophyll appears to depend on the seasonal availability of light, since the biomes are similarly nutrient limited. In these biomes, shoaling the euphotic zone concentrates phytoplankton closer to the surface. In equatorial and low-latitude regions, the steady supply of light and upwelling currents keep phytoplankton near the surface mostly year-round. Here, surface chlorophyll increased by 21 to 24 %. In the permanently stratified biome, there are intermittent mixing events and, on average, downwelling currents. Mixing the phytoplankton throughout the water column has the effect of reducing the concentration of phytoplankton near the surface. Any increases in surface chlorophyll in the stratified regions will be intermittent and by annual average smaller than the changes found near the equator, which explains why surface chlorophyll increased by 15 % in the permanently stratified biome.

3.4 Coastal regions and model error

The spatial distribution of light absorption by CDM in Fig. 7 and diminished attenuation depth in Fig. 8 suggest the addition of CDM to the optical model would have a significant impact on ocean productivity in coastal regions. For the following analysis, the coastal region was defined as grid cells adjacent to land.

In coastal regions, surface nutrients increased by 16 %, surface biomass by 22 % and surface chlorophyll by 35 %. Depth-integrated trends were of the opposite sign compared to surface trends. Total biomass decreased by 18 % and total chlorophyll decreased by 17 % when CDM was included. The largest percentage change in integrated biomass was found in the equatorial latitudes, where there was up to a 38 % drop in coastal biomass. High northern latitudes north of 60° N experienced 17–36 % decreases in coastal biomass. Relative changes in depth-integrated coastal biomass are shown by latitude in Fig. 18. These results are reported with the understanding that the coastal circulation is likely to be poorly resolved in our coarse model. Nonetheless, they highlight the potential impact of including the optical impact of CDM in coastal regions.

The results shown in this paper compare the “chl&CDM” and “chl-only” model runs. A comparison of the output of the “chl&CDM” model run and a model run with the original

k_d parameterization, Eq. (3), show qualitatively similar trends in coastal regions. Surface nutrients increased by 1 %, surface biomass by 3 % and surface chlorophyll by 6 %, while depth-integrated biomass and chlorophyll decreased by 9 % ("chl&CDM" minus model run using Eq. (3)). It will be important for models to include the optical impact of CDM to avoid the potential error of misrepresenting light attenuation as models with finer grid resolution are developed, especially in coastal regions.

A similar comparison of the model runs using the "chl&CDM" and the original k_d parameterization, Eq. (3), for the entire ocean shows small changes in globally averaged surface and total nutrients, biomass and chlorophyll. Surface nutrients decreased by 3 %, surface biomass decreased by 2 % and surface chlorophyll decreased by 3 %. Total biomass increased by 1 % and total chlorophyll increased by less than 1 % when CDM was included. The differences in attenuation depth between "chl&CDM" and the original k_d parameterization are between 0 m to 2 m for large areas of the ocean, as shown in Fig. 19. As mentioned in the Methodology section, the chlorophyll term has a smaller coefficient and exponent in Eq. (5) compared to Eq. (3). Separating the optical contribution of chlorophyll and CDM into two terms gave less weight to the chlorophyll term. In some regions with little attenuation by CDM, there was decreased surface attenuation in the model run that included CDM due to the decreased attenuation by the chlorophyll term. As a result, there are more areas where the difference in attenuation is equal to or greater than 0, which can be seen in a comparison of Fig. 19 and Fig. 8, panel (a). The attenuation depth increased by an average of 0.9 m in locations where the difference in attenuation depth was positive. Based on these results, we find that the biological model error from explicitly excluding the optical impact of CDM by using Eq. (3) to be small for the open ocean. The biological implication for ESMs using Eq. (3) is most profound for coastal regions, as described in the previous paragraph.

4 Conclusions

This paper addressed the impact of colored detrital matter on biological production by altering the ~~visible~~ attenuation of the in-water light field in the GFDL CM2Mc Earth System Model with BLING biogeochemistry. Light absorption by detrital matter and CDOM, a_{dg}, was prescribed using a satellite dataset with near-complete global surface ocean coverage. Results show that increasing light limitation can decouple surface trends in modeled biomass and macronutrients. Although increased biomass is usually associated with high productivity and decreased nutrients, this was not the case in our light-limited model runs. Surface chlorophyll, biomass and nutrients all increased together. These changes can be attributed to ~~the movement of biological productivity higher up the water column, which increases~~ increased biological productivity in the upper water column and decrease below, which increased surface chlorophyll and biomass while simultaneously decreasing depth-integrated biomass. ~~Meanwhile,~~ The diminished total biomass ~~leaves~~ left excess nutrients in the water column that ~~are~~ were eventually delivered to the surface, elevating surface macronutrient concentrations. While absolute changes in chlorophyll and macronutrient concentrations were small, one key ~~qualitative outcome~~ implication of this model experiment is that surface biomass trends may not reflect how light limitation is reducing ecosystem productivity. Understanding changes in ecosystem productivity requires both surface and depth-resolved information.

Adding the optical impact of CDM decreased integrated coastal biomass and chlorophyll concentration by 18 %. Meanwhile, surface chlorophyll concentration in coastal regions increased by 35 %. The open ocean biome analysis showed how, in the BLING model, changes in surface chlorophyll and biomass over the upper 200 m in various biomes depend on a combination of light and nutrient availability. In the high latitudes, adding CDM to the light-only limited Northern Hemisphere vs. the iron-light colimited Southern Hemisphere seemed to have different impacts on biomass decline. In the low- to mid-latitudes, the ~~circulation patterns and its impact~~ impact of circulation on light availability ~~determines~~ for phytoplankton determined the structure of the chlorophyll profile and the response of that

biome to a shrinking euphotic zone. These results highlight the biomes that may be most vulnerable to changes in biomass and chlorophyll if met with changes in light availability. For example high-latitude biomes that were already light limited experienced the greatest drop in biomass from additional light limitation.

In this study, the k_d parameterization was developed with measurements from several major regions of the global oceans but did not comprehensively represent the entire ocean's optical properties. The model results showed greatest changes in biomass in the Northern Hemisphere polar and subpolar regions, but our parameterization did not include in situ data from these regions. The spatial distribution of a_{dg} was fixed, so it could not respond to changes in the light field as chlorophyll concentration is able to do in the CM2Mc-BLING coupled physical-biogeochemical model configuration. The a_{dg} values were constant with time so the seasonal cycle was not represented. ~~Analysis~~ An analysis of satellite monthly climatology data shows there is more variability near river mouths and equatorial upwelling zones (not shown), indicating these areas would be most affected by including annual cycles. Furthermore, surface values were held constant throughout the water column. Resolving these simplifications may have important impacts. An interactive CDOM tracer would be best suited for such a task, once the mechanisms that control the production and degradation of CDM are better understood. Previous work has elucidated some potential sources and sinks of CDOM to the ocean, including in situ production by heterotrophic microbial activity (Nelson et al., 2004), delivery by freshwater input from terrestrial sources and degradation by photobleaching when exposed to intense light conditions (Blough and DelVecchio, 2002). Recently, Nelson et al. (2010) showed the depth-resolved cross-sections of a_{CDOM} through the major ocean basins approximately follow apparent oxygen utilization contours. This suggests that oxygen might be used to improve modeling depth-dependent CDOM distributions in the future. Direct modeling of CDOM would be of particular importance to regions where CDOM abundance is in flux due to changes in the volume and composition freshwater runoff. In the Arctic Ocean, CDOM is of primary importance in determining the non-water absorption coefficient of light and its relatively concentrated presence increases energy absorbed in the mixed layer by trapping incoming

shortwave radiation (Pegau, 2002). Hill (2008) used a radiative transfer model to find the absorption of shortwave radiation by CDOM can increase energy absorbed by the mixed layer by 40 % over pure seawater and this additional energy can account for 48 % of springtime ice melt by water column heating. These impacts should be incorporated into future earth system models and existing higher resolution regional models to more accurately simulate the ocean heat budget and marine biogeochemistry.

Acknowledgements. This work was supported by NASA Headquarters under the NASA Earth and Space Science Fellowship Program – Grant NNX14AK98H. We thank contributors to the NASA SeaBASS data archive which made this work possible.

References

Blough, N. V. and DelVecchio, R.: Chapter 10: Chromophoric DOM in the Coastal Environment, in: Biogeochemistry of Marine Dissolved Organic Matter, edited by: Hansell, D. A., and Carlson, C. A., Academic Press, San Diego, 509–546, doi:10.1016/B978-012323841-2/50012-9, 2002.

Dunne, J. P., Armstrong, R. A., Gnanadesikan, A., and Sarmiento, J. L.: Empirical and mechanistic models for the particle export ratio, Global Biogeochem. Cy., 19, GB4026, doi:10.1029/2004GB002390, 2005.

Dutkiewicz, S., Hickman, A. E., Jahn, O., Gregg, W. W., Mouw, C. B. and Follows, M. J.: Capturing optically important constituents and properties in a marine biogeochemical and ecosystem model, Biogeosciences Discuss., 12, 2607–2695, doi:10.5194/bgd-12-2607-2015, 2015.

Eppley, R.: Temperature and phytoplankton growth in the sea, Fishery Bulletin, 70, 1063–1085, 1972.

Galbraith, E. D., Gnanadesikan, A., Dunne, J. P., and Hiscock, M. R.: Regional impacts of iron-light colimitation in a global biogeochemical model, Biogeosciences, 7, 1043–1064, doi:10.5194/bg-7-1043-2010, 2010.

Galbraith, E. D., Kwon, E. Y., Gnanadesikan, A., Rodgers, K. B., Griffies, S. M., Bianchi, D., Sarmiento, J. L., Dunne, J. P., Simeon, J., Slater, R. D., Wittenberg, A. T., and Held, I. M.: Climate Variability and Radiocarbon in the CM2Mc Earth System Model., J. Climate, 24, 4230–4254, 2011.

Garcia, H. E., Locarnini, R. A., Boyer, T. P., Antonov, J. I., Baranova, O., Zweng, M., Reagan, J., and Johnson, D.: World Ocean Atlas 2013, Volume 4: Dissolved Inorganic Nutrients (phosphate, nitrate, silicate), NOAA Atlas NESDIS 76, edited by: Levitus, S. and Mishonov, A., 2014.

Gnanadesikan, A. and Anderson, W. G.: Ocean water clarity and the ocean general circulation in a coupled climate model., J. Phys. Oceanogr., 39, 314–332, 2009.

Gregg, W. W. and Casey, N. W.: ~~Skill assessment of a spectral ocean–atmosphere radiative model, J. Marine Syst.~~ Modeling coccolithophores in the global oceans, Deep Sea Res. Pt. II, 54, 447–477, ~~76, 49–63,~~ doi:~~, 2009.~~10.1016/j.dsr2.2006.12.007, 2007.

Hill, V. J.: Impacts of chromophoric dissolved organic material on surface ocean heating in the Chukchi Sea, J. Geophys. Res.-Oceans, 113, C07024, doi:10.1029/2007JC004119, 2008.

Manizza, M., Le Quéré, C., Watson, A. J., and Buitenhuis, E. T.: Bio-optical feedbacks among phytoplankton, upper ocean physics and sea-ice in a global model, Geophys. Res. Lett., 32, L05603, doi:10.1029/2004GL020778, 2005.

Morel, A.: Optical modeling of the upper ocean in relation to its biogenous matter content (case I waters), J. Geophys. Res.-Oceans, 93, 10749–10768, doi:10.1029/JC093iC09p10749, 1988.

Murtugudde, R., Beauchamp, J., McClain, C. R., Lewis, M., and Busalacchi, A. J.: Effects of penetrative radiation on the upper tropical ocean circulation., J. Climate, 15, 470–486, 2002.

Nelson, N. B. and Siegel, D. A.: The global distribution and dynamics of chromophoric dissolved organic matter, Annual Review of Marine Science, 5, 447–476, doi:10.1146/annurev-marine-120710-100751, pMID: 22809178, 2013.

Nelson, N. B., Carlson, C. A., and Steinberg, D. K.: Production of chromophoric dissolved organic matter by Sargasso Sea microbes, Mar. Chem., 89, 273–287, doi:10.1016/j.marchem.2004.02.017, 2004.

Nelson, N. B., Siegel, D. A., Carlson, C. A., and Swan, C. M.: Tracing global biogeochemical cycles and meridional overturning circulation using chromophoric dissolved organic matter, Geophys. Res. Lett., 37, L03610, doi:10.1029/2009GL042325, 2010.

Ohlmann, J. C. and Siegel, D. A.: Ocean radiant heating. Part II: Parameterizing solar radiation transmission through the upper ocean, J. Phys. Oceanogr., 30, 1849–1865, doi:10.1175/1520-0485(2000)030<1849:ORHPIP>2.0.CO;2, 2000.

Pegau, W. S.: Inherent optical properties of the central Arctic surface waters, J. Geophys. Res.-Oceans, 107, SHE 16-1–SHE 16-7, doi:10.1029/2000JC000382, 2002.

Pope, R. M. and Fry, E. S.: Absorption spectrum (380-700nm) of pure water. II. Integrating cavity measurements, Appl. Opt., 36:8710–8723., doi:10.1364/AO.36.008710, 1997.

Reynolds, R. W., Rayner, N. A., Smith, T. M., Stokes, D. C., Wang, W.: An improved in situ and satellite SST analysis for climate, J. Climate, 15:1609–1625., doi:10.1175/1520-0442(2002)015<1609:AIISAS>2.0.CO;2, 2002.

Sarmiento, J. L. and Gruber, N.: Ocean Biogeochemical Dynamics, Princeton University Press, Princeton, New Jersey, 2006.

Sarmiento, J. L., Slater, R., Barber, R., Bopp, L., Doney, S. C., Hirst, A. C., Kleypas, J., Matear, R., Mikolajewicz, U., Monfray, P., Soldatov, V., Spall, S. A., and Stouffer, R.: Response of ocean ecosystems to climate warming, Global Biogeochem. Cy., 18, GB3003, doi:10.1029/2003GB002134, 2004.

Siegel, D. A., Maritorena, S., Nelson, N. B., and Behrenfeld, M. J.: Independence and interdependencies among global ocean color properties: reassessing the bio-optical assumption, J. Geophys. Res.-Oceans, 110, C07011, doi:10.1029/2004JC002527, 2005.

Werdell, P. J. and Bailey, S. W.: An improved in-situ bio-optical data set for ocean color algorithm development and satellite data product validation, Remote Sens. Environ., 98, 122–140, doi:10.1016/j.rse.2005.07.001, 2005.

Yoder, J. A. and Kennelly, M. A.: Seasonal and ENSO variability in global ocean phytoplankton chlorophyll derived from 4 years of SeaWiFS measurements, Global Biogeochem. Cy., 17, 23-1–23-14, doi:10.1029/2002GB001942, 2003.

Table 1. Surface area by biome, in km^2 with percentage change in area between the two model runs (chl&CDM minus chl-only).

Biome	chl&CDM	% age of total	chl-only	% age of total	% change
Equatorial Upwell	1.86×10^7	6 %	1.86×10^7	6 %	0 %
Equatorial Downwell	8.34×10^6	3 %	8.07×10^6	3 %	3 %
Low Latitude Upwell	6.32×10^7	21 %	6.32×10^7	21 %	0 %
Permanently Stratified	1.01×10^8	34 %	9.89×10^7	33 %	2 %
Seasonally Stratified	3.93×10^7	13 %	4.11×10^7	14 %	−4 %
Subpolar NH	1.22×10^7	4 %	1.35×10^7	4 %	−9 %
Ice NH	1.17×10^7	4 %	9.81×10^6	3 %	19 %
Subpolar SH	2.33×10^7	8 %	2.43×10^7	8 %	−4 %
Ice SH	2.37×10^7	8 %	2.27×10^7	8 %	4 %

Table 2. Difference in surface chlorophyll $\mathrm{mg\,m^{-3}}$, biomass $\mathrm{mg\,C\,m^{-3}}$ and macronutrient µM concentrations, chl&CDM minus chl-only. Surface values are the average over the top 10 m. All surface changes are statistically significant to three ~~SDs~~standard deviations. Statistical significance tests were performed on decadally smoothed data from the the final 100 years of the two model runs.

Biome	Δ chl	% Δ	Δ biomass	% Δ	Δ nutrient	% Δ
Equatorial Upwell	0.28	22 %	4.5	16 %	0.053	14 %
Equatorial Downwell	0.23	24 %	4.2	17 %	0.052	24 %
Low Latitude Upwell	0.21	21 %	3.1	15 %	0.038	20 %
Permanently Stratified	0.18	15 %	2.0	10 %	0.036	13 %
Seasonally Stratified	0.52	7 %	2.2	5 %	0.066	15 %
Subpolar NH	0.83	9 %	4.2	7 %	0.071	19 %
Ice NH	0.90	18 %	7.7	14 %	0.10	23 %
Subpolar SH	0.29	7 %	0.97	3 %	0.041	3 %
Ice SH	0.18	11 %	1.3	6 %	0.038	2 %

Table 3. Difference in chlorophyll $\mathrm{mg\,m^{-2}}$, biomass $\mathrm{mg\,C\,m^{-2}}$ and macronutrients $\mathrm{mmol\,m^{-2}}$ between the two model runs (chl&CDM minus chl-only), integrated over the upper 200 m.

Biome	Δ chl	% Δ	Δ biomass	% Δ	Δ nutrient	% Δ
Equatorial Upwell	−1.7	−7 %	−87	−6 %	15	8 %
Equatorial Downwell	−1.2	−5 %	−67	−5 %	17	11 %
Low Latitude Upwell	−0.74	−4 %	−38	−3 %	13	9 %
Permanently Stratified	−0.77	−4 %	−61	−4 %	11	11 %
Seasonally Stratified	−2.2	−5 %	−127	−5 %	16	13 %
Subpolar NH	−8.8	−14 %	−482	−15 %	15	11 %
Ice NH	−2.2	−5 %	−179	−8 %	22	16 %
Subpolar SH	−1.6	−5 %	−139	−6 %	7.4	2 %
Ice SH	−2.1	−9 %	−165	−10 %	5.3	1 %

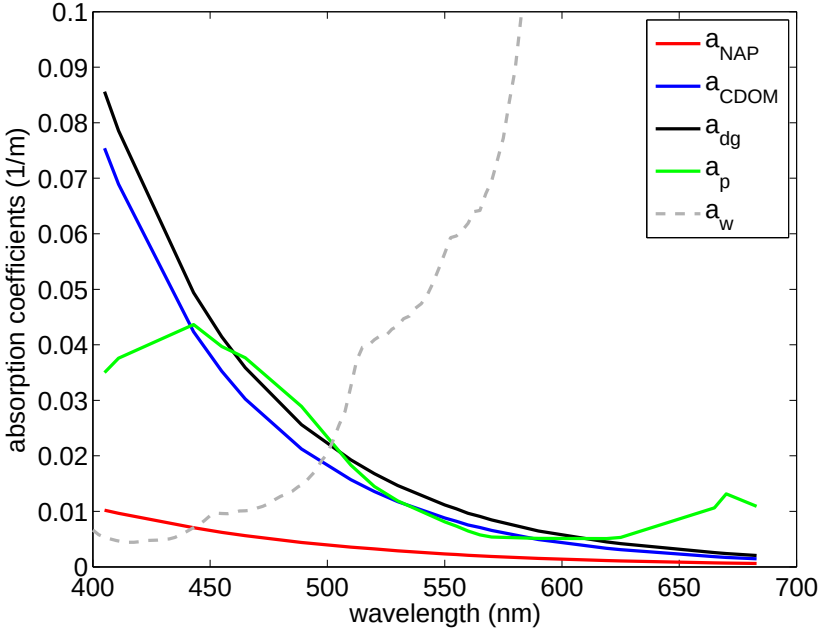

Figure 1. Median IOP spectra from NOMAD dataset and absorption spectrum of pure water in gray. In the visible spectrum, CDOM absorption is strongest in the blue and decreases exponentially with increasing wavelength. The absorption spectrum of pure water is 0.0434 m^{-1} at 530nm and increases to 0.6 m^{-1} at 700nm, exceeding the axis limits shown here. (Pope and Fry, 1997) The absorption spectrum of particles (including phytoplankton), a_p, absorbs strongly in the red wavelengths compared to NAP and CDOM.

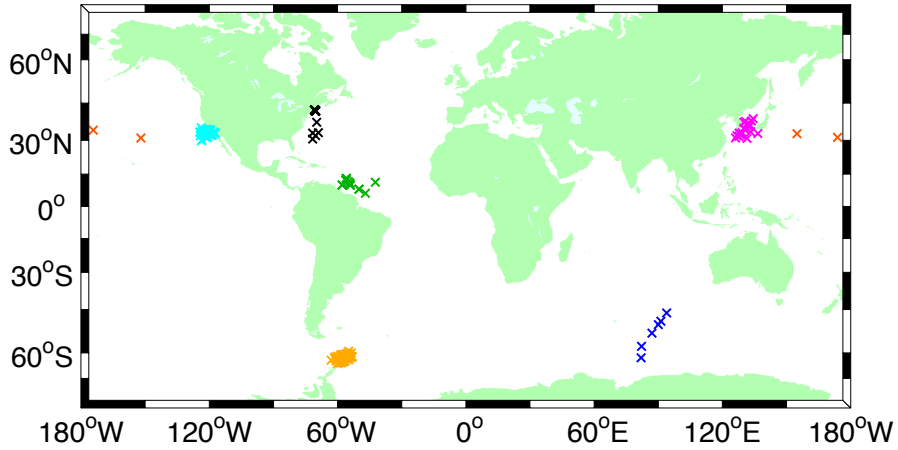

Figure 2. ~~(a)~~ Map of stations with locations of the 244 in-situ measurements used to develop the $k_{\mathrm{d}}(\mathrm{bg})$ parameterization with CDM, Eq. (5)~~(b) comparison of Eqs.~~, color coded by arbitrarily grouped by region: (~~3~~1) western Atlantic, northern cluster in black; (2) western Atlantic, Amazon river outflow and offshore stations in green; (~~5~~3) ~~applied to NOMAD~~ Antarctic peninsula in ~~situ chlorophyll concentration~~ orange; (4) Southern Ocean in blue; (5) western Pacific in magenta; (6) stations across the Pacific ocean in red and $a_{\mathrm{dg}}(443)$ ~~measurements to calculate $k_{\mathrm{d}}(\mathrm{bg})$~~(7) eastern Pacific in cyan.~~The 0.88 slope on the regression line indicates that when CDM is included, $k_{\mathrm{d}}(\mathrm{bg})$ increases more rapidly than when it depends on chlorophyll concentration alone.~~

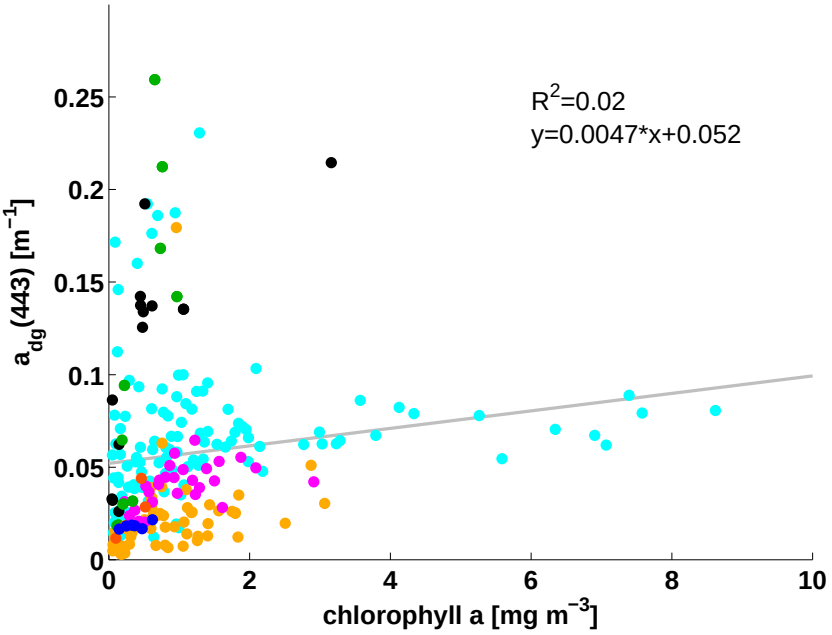

Figure 3. Scatterplot of 244 in-situ chlorophyll-a concentration and $a_{dg}(443)$ concurrent measurements from the NOMAD dataset used to develop the $k_d(bg)$ parameterization with CDM, Eq. (5). Color coding corresponds to regional groupings from Fig. 2.

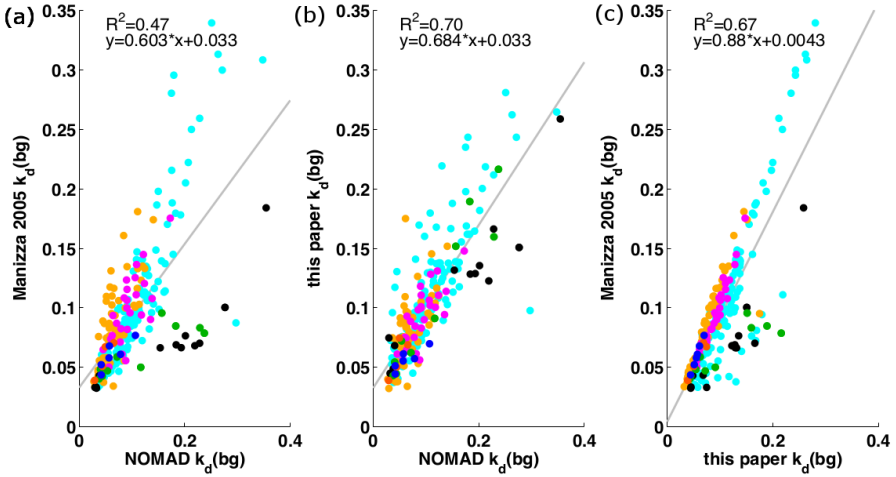

Figure 4. **(a)** and **(b)** Scatterplots comparing observed k_d(bg) from the NOMAD dataset and modeled k_d(bg) using two different parameterizations, Eqs. (3) and (5). The modeled k_d(bg) values are calculated from in situ chlorophyll-a and a_{dg}(443) measurements corresponding to the observed k_d(bg) values on the x-axis. **(c)** Comparison of Eqs. (3) and (5) applied to NOMAD in situ chlorophyll concentration and a_{dg}(443) measurements to calculate k_d(bg). The 0.88 slope on the regression line indicates that when CDM is included, k_d(bg) increases more rapidly than when it depends on chlorophyll concentration alone. Color coding corresponds to regional groupings from Fig. 2.

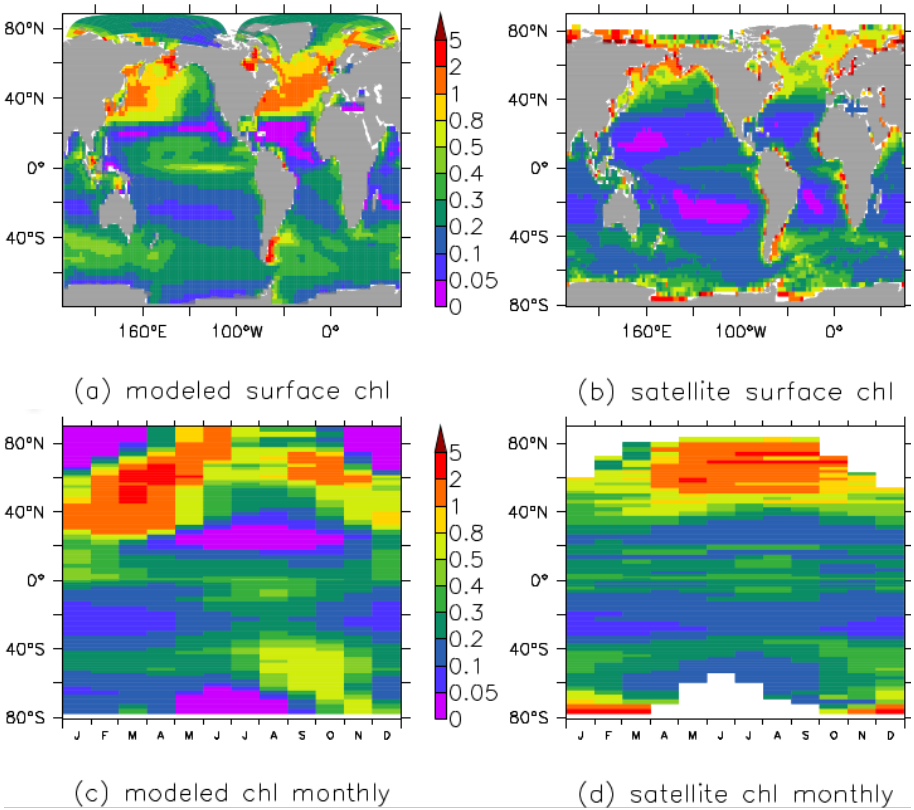

Figure 5. Comparison of **(b, d)** chlorophyll concentration in mg m^{-3} from SeaWiFS satellite observation (Yoder and Kennelly, 2003) used in earlier similar studies and **(a, c)** modeled using GFDL ESM CM2Mc with BLING biogeochemistry. Data shown are from the chl&CDM model run described in Sect. 4 of this paper. Annual average surface distributions are shown in **(a, b)** and monthly average surface concentration by latitude are shown in **(c, d)**.

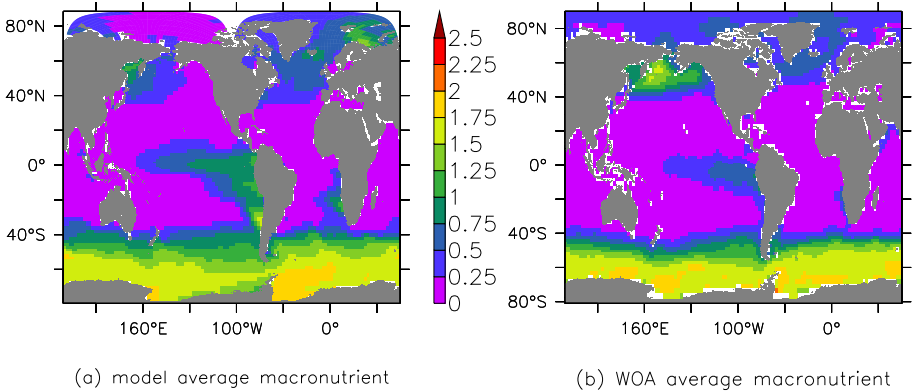

Figure 6. Comparison of **(a)** modeled using GFDL CM2Mc with BLING biogeochemistry and **(b)** measured macronutrient concentration, $\frac{1}{2}(PO_4 + \frac{NO_3}{16})$, from World Ocean Atlas 2013 nitrate and phosphate datasets (Garcia et al., 2014). Concentration in µM~~(Garcia et al., 2014)~~.

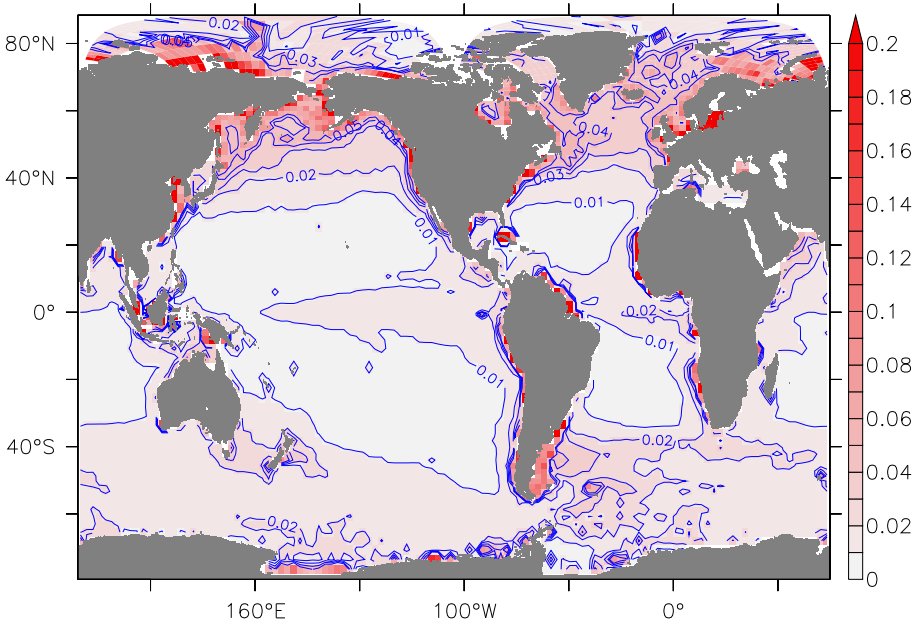

Figure 7. The spatial distribution of $a_{\mathrm{dg}}(443)$ as prescribed in the model runs for this paper, mapped onto the CM2Mc ESM tracer grid with data extrapolated into polar regions.

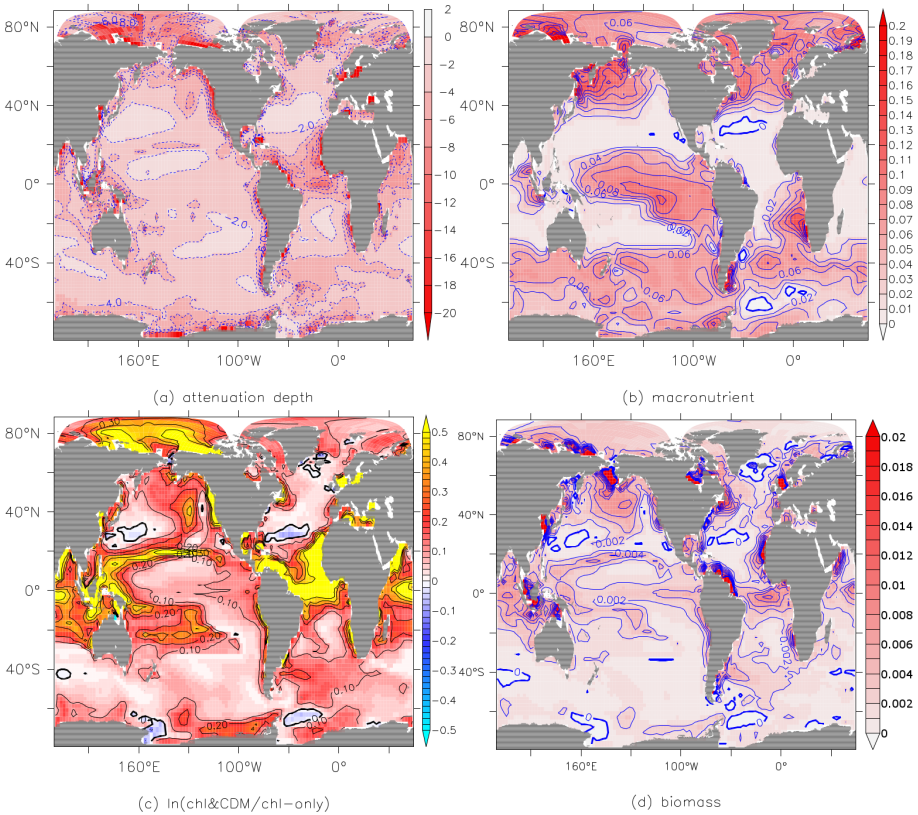

Figure 8. Difference **(a)** attenuation depth m, **(b)** surface macronutrient concentration µM, **(c)** surface chlorophyll concentration and **(d)** surface biomass concentration g C m^{-3}; chl&CDM minus chl-only. Surface values represent the average over the top 10 m. Panel **(c)** shows natural log ratio of chlorophyll concentration from the chl&CDM run over chl-only run, so positive values indicate an increase in chlorophyll in the chl&CDM run.

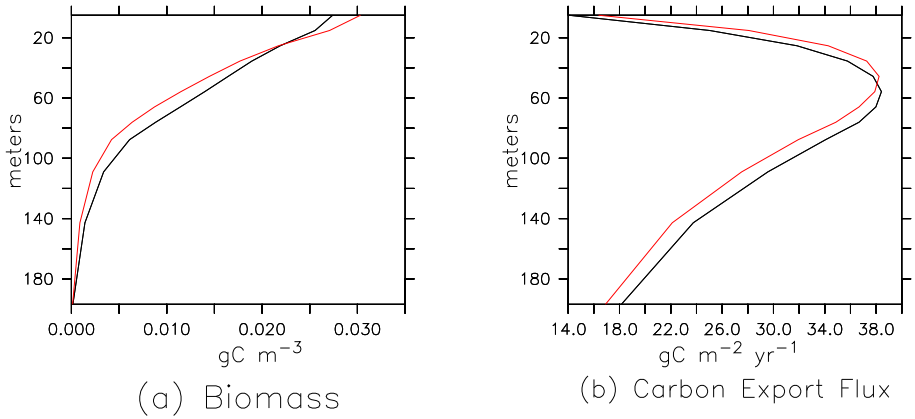

Figure 9. Globally averaged profile of **(a)** biomass in $\mathrm{g\,C\,m^{-3}}$ and **(b)** carbon export flux in $\mathrm{g\,C\,m^{-2}\,yr^{-1}}$. Black line shows data from the chl-only run, red line represents chl&CDM run.

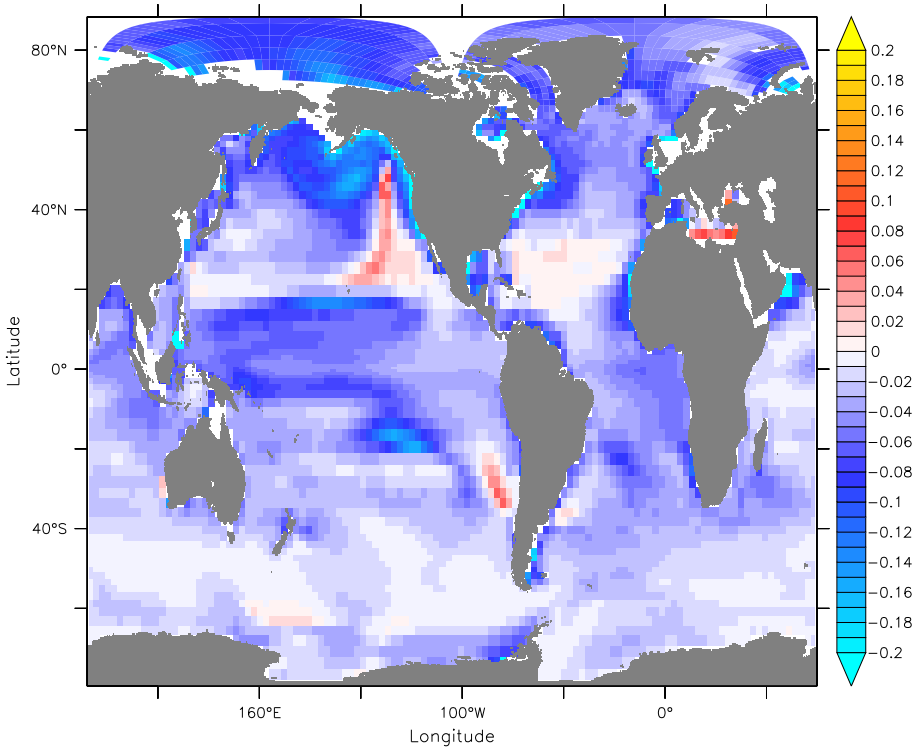

Figure 10. Difference in E_{bp}, chl&CDM model run minus chl-only model run.

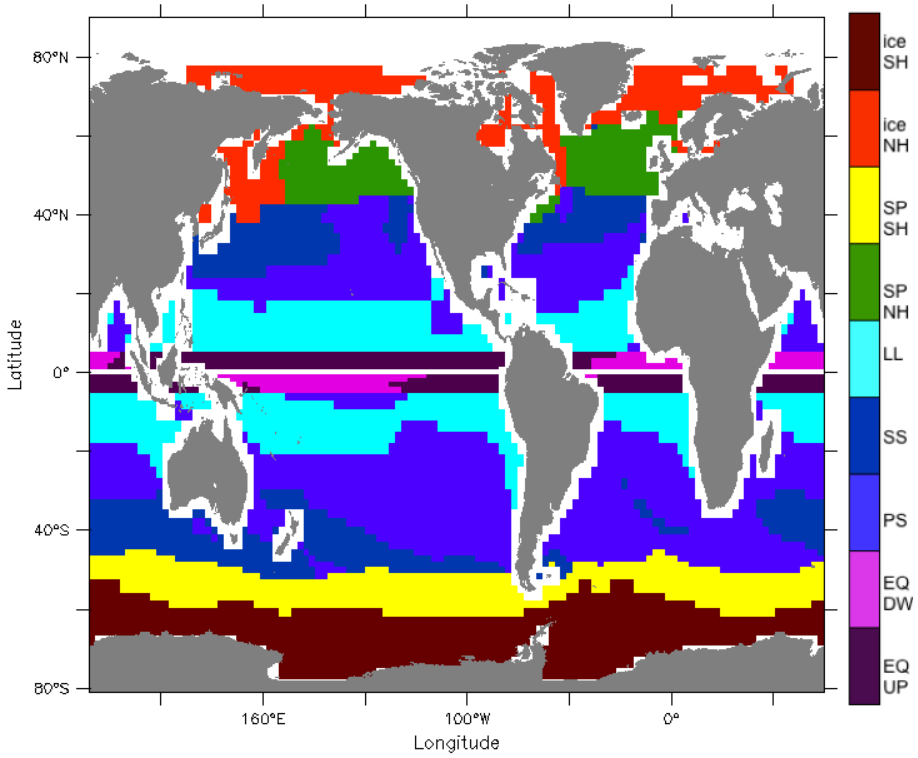

Figure 11. Biomes as defined by Sarmiento et al. (2004) applied to GFDL CM2Mc with chl&CDM k_{d} parameterization, Eq. (5). Legend abbreviations: ice = marginal ice zone, SP = subpolar, LL = lower latitude, SS = seasonally stratified, PS = permanently stratified, EQ DW = equatorial downwelling, EQ UP = equatorial upwelling. Suffixes NH and SH stand for northern hemisphere and southern hemisphere.

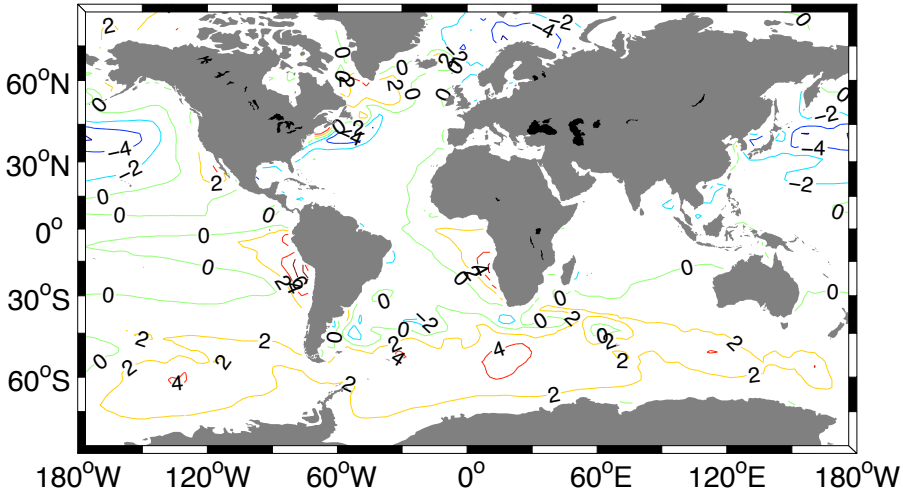

Figure 12. ~~Percent change~~ Difference in ~~total integrated biomass~~ annual average SST in ~~coastal regions~~°C, ~~by latitude~~chl&CDM minus observed using the NOAA_OI_SST_V2 dataset (Reynolds, 2002).~~Coastal regions are defined as model grid boxes adjacent to land.~~

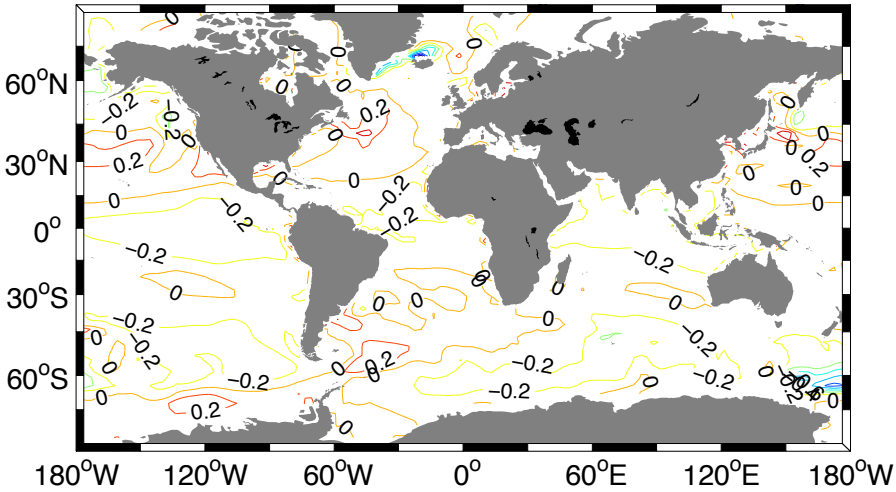

Figure 13. Difference in annual average SST in °C, chl&CDM minus chl-only.

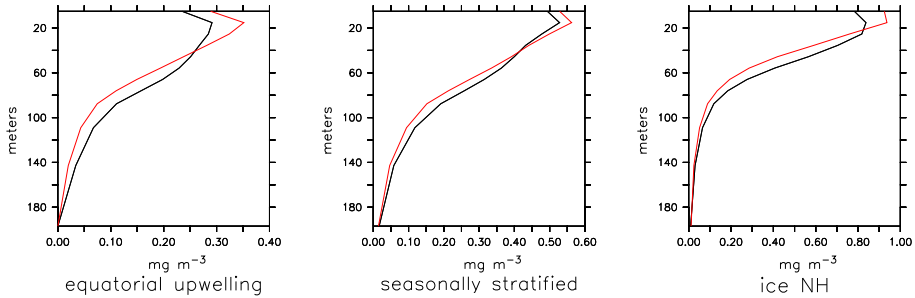

Figure 14. The depth profile of chlorophyll concentration $\mathrm{mg\,m^{-3}}$ in three biomes. The black line indicates the chl-only run, red line represents chl&CDM run. The equatorial upwelling and seasonally stratified biomes show increased peaks in the deep chlorophyll maximum (DCM) when CDM is included. All three biomes show increased chlorophyll near the surface, but diminished chlorophyll at depth.

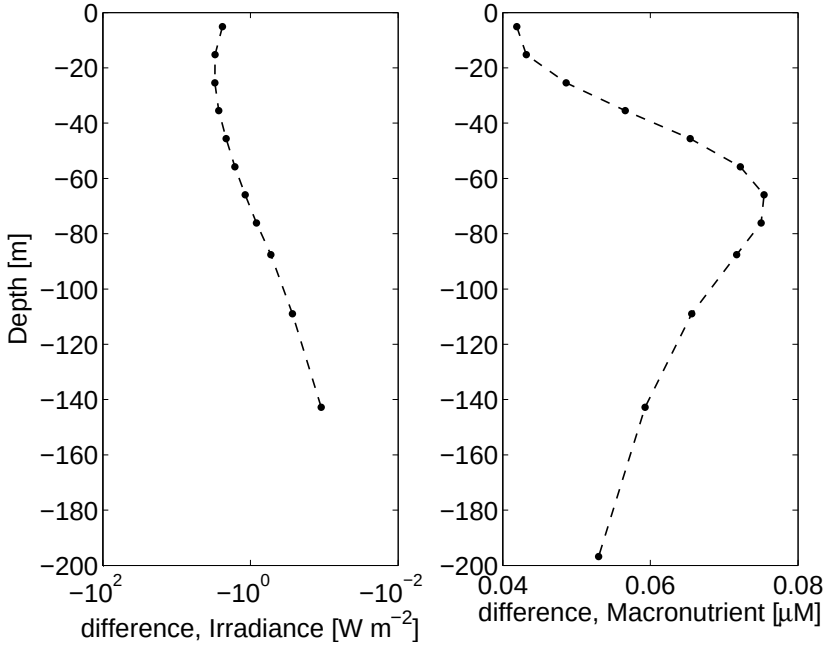

Figure 15. Profiles of ~~percent change~~ the difference in globally averaged irradiance and macronutrient concentration, ~~chl-only minus~~ chl&CDM minus chl-only. There is a decrease in irradiance and increase in macronutrients throughout the upper 200 m. The ~~percentage~~ difference in irradiance ~~is 0~~ at ~~200 because 200~~ 196m is ~~the model-prescribed maximum light penetration depth~~zero.

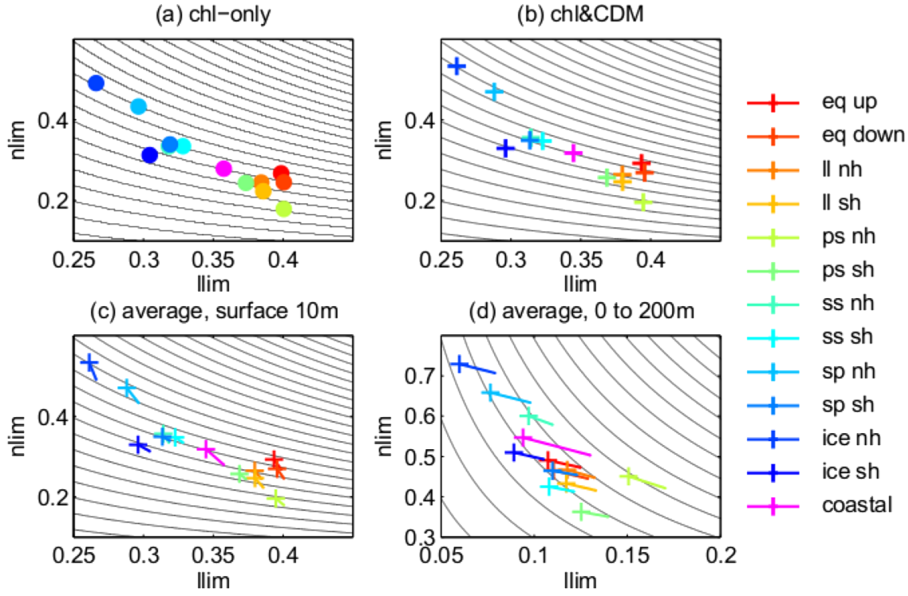

Figure 16. Light and nutrient limitation scaling factors for open ocean biomes and coastal regions. **(a)** Average nlim, llim for chl-only model run, from 0 to 10 m **(b)** average nlim, llim for chl&CDM model run, from 0 to 10 m **(c)** vectors connecting coordinates from panel **(a, b)**, average from 0 to 10 m. **(d)** Vectors starting at coordinates from chl-only model run and terminating with an "x" at values from chl&CDM model run, average from 0 to 200 m. Legend abbreviations: ice = marginal ice zone, sp = subpolar, ss = seasonally stratified, ps = permanently stratified, ll = lower latitude, ~~equp~~eq up = equatorial upwelling, ~~eqdown~~eq down = equatorial downwelling, coastal = coastal regions, defined as the grid cells adjacent to land. Suffixes nh and sh stand for Northern Hemisphere and Southern Hemisphere.

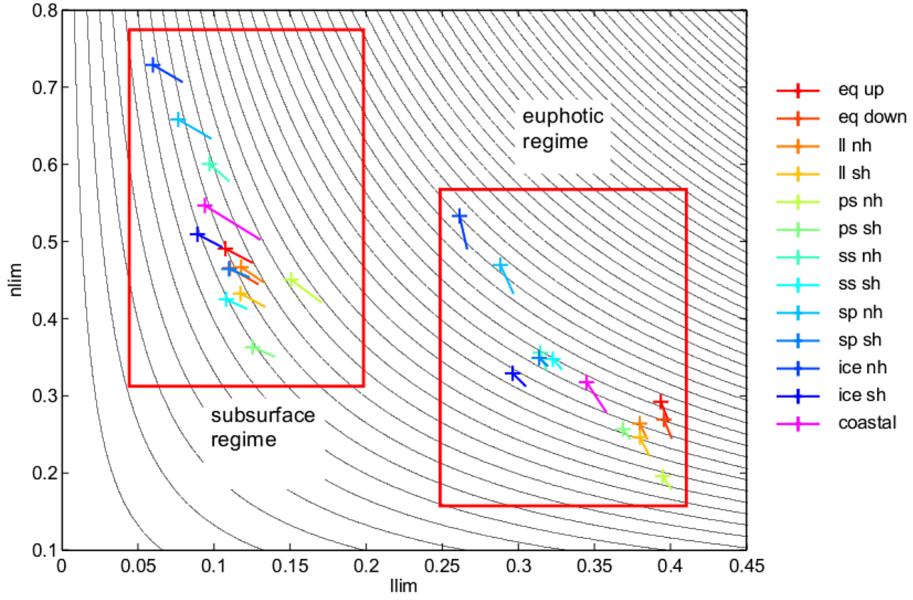

Figure 17. All vectors from Fig. 16c and d, on the same plot. Vectors for nlim, llim values averaged over the upper 10 m occupy the "euphotic regime" and values averaged over the upper 200 m occupy the "subsurface regime".

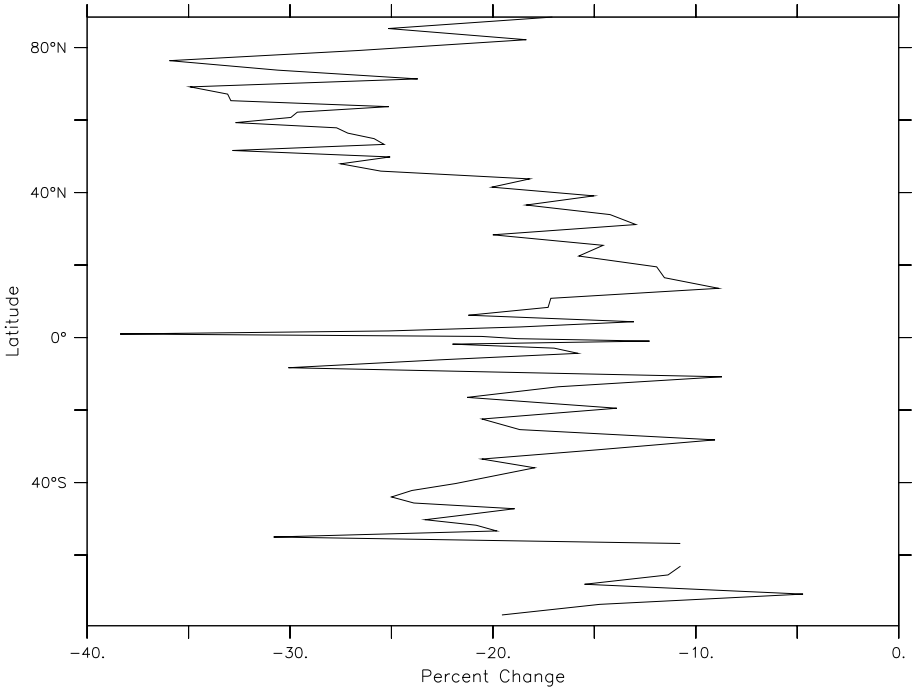

Figure 18. Percent change in total integrated biomass in coastal regions, by latitude. Coastal regions are defined as model grid boxes adjacent to land.

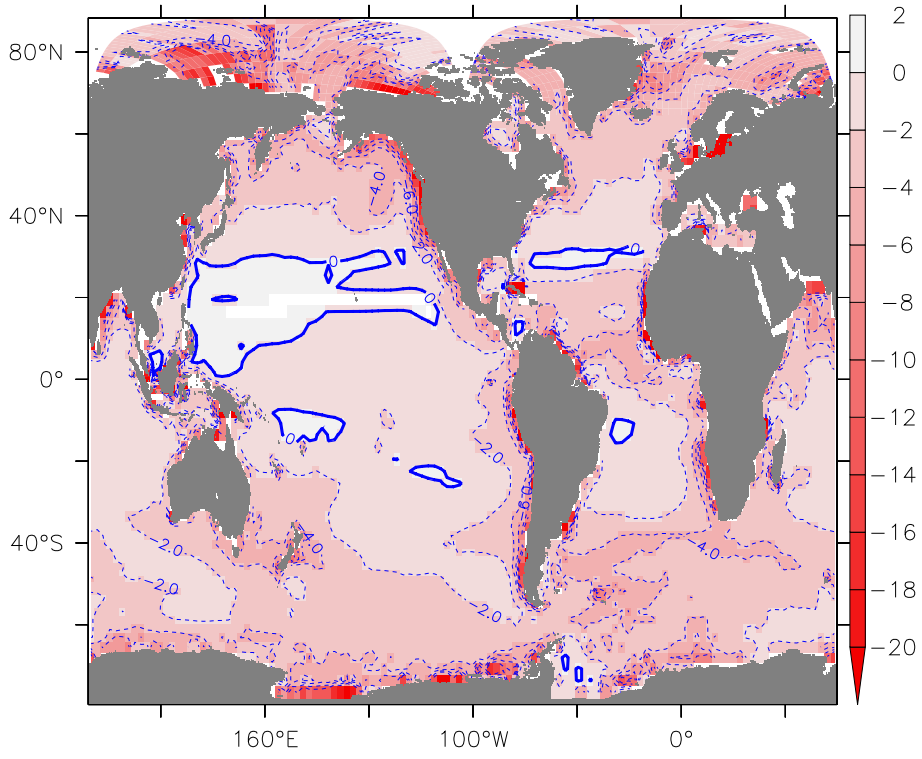

Figure 19. Difference in attenuation depth in m; chl&CDM minus model run using Eq. (3).